KERNFORSCHUNGSZENTRUM

KARLSRUHE
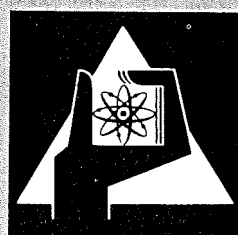
Physics Investigations of Two Pu-Fueled Fast Critical Assemblies:
SNEAK-7A and 7B

compiled
E.A. Fischer, P.E. McGrath

Physics Investigations of Two Pu-Fueled

Fast Critical Assemblies:

SNEAK-7A and 7B

Compiled by

E.A. Fischer and P.E. Mc Grath

With contributions from

W. Bickel, R. Böhme, R. Buyl, P. Fehsenfeld, E. Korthaus,
W.J. Oosterkamp, R. Papp, M. Pinter, W. Scholtyssek,
O. Sotic, W. Väth, H. Walze, G. Wittek

Physics Investigations of Two Pu-Fueled

Fast Critical Assemblies:

SNEAK-7A and 7B

Abstract

Two Pu-fueled fast critical assemblies of different enrichment
were studied in the Karlsruhe Fast Critical Facility SNEAK for
the purpose of testing cross section data and calculational
methods. The measurements suitable for such purpose are cen-
tral reaction rates and reactivity worths. To investigate the
discrepancy in the reactivity scale of fast reactors measure-
ments of the normalization integral and β_{eff} were performed.
In addition, measurements of the core material buckling, which
characterizes the core material independent of its geometry
and environment, were also included.

The measurement procedures employed are described in some de-
tail. The evaluation of the measurements was performed with
the most recent cross section sets and computer codes avail-
able at Karlsruhe. Some of the evaluations were also performed
with a cross section set based on ENDF/B data.

3.5.1974

Physikalische Untersuchungen an zwei schnellen

kritischen Plutonium-Anordnungen:

SNEAK-7A und 7B

Zusammenfassung

In der Schnellen Null-Energie-Anlage Karlsruhe (SNEAK) wurden
zwei einfache Anordnungen mit Mischoxid verschiedener Anrei-
cherungen als Brennstoff untersucht. Der Zweck dieser Unter-
suchungen war die Überprüfung von Querschnittsdaten und Re-
chenmethoden. Die dafür geeigneten Messungen sind Ratenver-
hältnisse und Materialwerte im Corezentrum. Außerdem wurde
das materielle Buckling experimentell bestimmt; es ist ein
charakteristischer Parameter der Core-Komposition und unab-
hängig von der Form des Cores und den Eigenschaften des Re-
flektors. Um eine Aussage über die mit großen Unsicherheiten
behaftete Reaktivitätsskala zu gewinnen, wurden β_{eff} und das
Normierungsintegral experimentell bestimmt.

Die Meßmethoden werden in einiger Ausführlichkeit beschrieben.
Die Nachrechnungen der Ergebnisse erfolgte mit den neuesten
Karlsruher Querschnittssätzen und Rechenprogrammen. Einige
Ergebnisse wurden zusätzlich mit Daten nachgerechnet, die
von ENDF/B abgeleitet wurden.

Table of Contents

Appendices

1. Introduction

The fast critical facility SNEAK /1/ (Schnelle Null-Energie-An-
ordnung Karlsruhe) was utilized during the first half of the
year 1971 to perform physics experiments on two clean plutonium
fueled fast assemblies. Both assemblies were simple one zone cores
fueled with PuO_2-UO_2 and reflected by depleted uranium. The aim
was to test cross section data and calculational methods used on
fast Pu-fueled cores, and in particular to investigate their con-
sistency for cases of different enrichments. The two assemblies
had compact cores of, respectively, 100 and 300 liters in volume
and similar hard spectra to emphasize the inelastic scattering
energy region of ^{238}U and to facilitate comparison between the
two assemblies.

The experiments performed in these two assemblies were central
reaction rates and reactivity worths. For the purpose of inves-
tigating the discrepancy of the reactivity scale in fast reac-
tors a measurement of the normalization integral was performed,
as well as several independent determinations of β_{eff}. Included
also were measurements of the core material buckling which char-
acterizes the core material independent of its geometry and
environment. The experimental procedures utilized for the meas-
urements are described in this report in some detail.

An evaluation of all the measurements was performed with the
two most recent Karlsruhe cross section sets. Some of the eval-
uations were also performed with a cross section set based on
recent ENDF/B data. Therefore the results reflect the current
state of the cross section data.

2. Basic Description of the Assemblies

SNEAK is a fixed vertical assembly with fuel elements suspended
from a grid plate. The SNEAK cores are composed of square plate-
lets which are stacked horizontally in vertical stainless steel
tubes. In one assembly, SNEAK-7A, the unit cell consisted of one
PuO_2UO_2 platelet (26.6% PuO_2 and 73.4% UO_2) and one graphite
platelet. In the other Pu assembly, SNEAK-7B, the graphite plate-
let in the cell of 7A was exchanged by a $U_{nat}O_2$ platelet giving
an average Pu-enrichment, in this case, of about 13%. Both assemb-
lies had a single core zone and a reflector of depleted uranium.

The material inventory of the SNEAK assembly includes only a
small fraction of the PuO_2-UO_2 special platelets necessary to
load all of the control rods with a composition identical to
the cores. Therefore it was necessary to load the control rods
with an enriched uranium cell. As a result approximately 10%
of the critical mass in both assemblies was ^{235}U. For the
homogeneous calculations the uranium control rods were homo-
genized over the assembly core zone.

A detailed description of the assemblies is given in Appendix A1.
Included is the RZ-two dimensional model used to analyze the
assemblies. The compositions of individual platelets of the
core zones are given as well as the homogeneous compositions.
In addition, in Appendix A2 a spherical model representation
of the two assemblies is given. These models may be used for
basic one-dimensional analysis of the assemblies. For this
purpose experimental results corrected for the spherical re-
presentation are provided.

3. Cross Section Data and Calculational Concepts

The development of cross section sets at Karlsruhe for the eval-
uation of fast reactors has followed from the well known Russian
ABN cross section set concept /2/. The concept involved is the
use of homogeneous composition dependent self-shielding factors
to describe the resonance self-shielding of each resonance ma-
terial in the composition. Although the procedure was introduced
many years ago it has only recently been tested extensively against
a more exact model by Kidman et al. /3/ and found to have suffi-
cient accuracy for most calculations. A consistent formulation
using self-shielding factors in heterogeneous media (multiregion
cells) was developed at Karlsruhe /4/ and is also used extensively
for the evaluation of experiments in SNEAK. This program, KAPER,
is capable of calculating the fine structure flux distributions
in the heterogeneous core cells while accounting for the resonance
self-shielding of the cross sections. This calculation capability
is used to evaluate reaction rate measurements in the cell (spec-
tral indices) since one measures with thin foils at a particular
position in the cell. In addition, the KAPER program is used to
calculate heterogeneous reactivity worths of small samples. The
KAPER description of the experimental arrangement represents a
significant improvement over the capabilities of homogeneous dif-
fusion theory. Therefore all of the calculated results presented
in this report, except where noted, are based on the "f-factor
concept".

For the evaluation of the measurements performed in the two SNEAK-7
assemblies, the two most recent Karlsruhe cross section sets, MOXTOT
and KFKINR, were utilized. The basic data used in the MOXTOT set are
documented in /5/ and those for the KFKINR set in /6/. The important
differences, for our purposes, between the MOXTOT and KFKINR sets
are the following:

i)   In all previous Karlsruhe cross section sets, including the
      MOXTOT set, the "Standard-Fission-Spectrum" of the ABN set
      was used. For the KFKINR set the fission spectrum is cal-
      culated for each particular composition from the contribu-
      tions of all the fissionable isotopes present in the com-
      position. The fission spectrum of each fissionable isotope
      is represented by a Maxwellian distribution.

ii)   In the KFKINR set the inelastic scattering cross section
      of ^{238}U is approximately 20% smaller than that in the
      MOXTOT set. In addition, the average energy loss per in-
      elastic scattering is smaller.

iii) The ^{239}Pu-alpha (capture-to-fission ratio) in the KFKINR
      set was increased slightly as well as the ^{239}Pu fission
      cross section.

iiii) The capture cross section of ^{238}U in the energy range of
      100 keV - 800 keV was increased for the KFKINR set.

These differences in the two cross section sets are reflected in
the results quoted in this report. In particular, the changes men-
tioned under point ii) have the largest influence on the calculated
results.

In addition to the two Karlsruhe cross section sets, a 26-group
cross section set based on ENDF/B data was utilized. This set was
derived from the 29-group set prepared by Kidman and Schenter /7/
with the ETOX-2 program and the ENDF/B (Version III) cross section
library. The modifications made at Karlsruhe were a condensation

of a few groups to be compatible with the Karlsruhe program system and a recalculation of the elastic slowing down cross sections with the weighting spectrum utilized in the KFKINR set.

4. Critical Experiment and Evaluation

The criticality of the two assemblies was determined with all control rods in their most reactive position, i.e. with the fueled portion of the rod in the core. With the SNEAK-7A core loaded as shown in Fig. A1-1 it was determined to be 29.6 ¢ supercritical. The SNEAK-7B core, loaded as shown in Fig. A1-3, was determined to be 40 ¢ supercritical. In SNEAK-7A the supercriticality of the core represents $1^o/oo$ in k_{eff} and in SNEAK-7B $1.6^o/oo$ in k_{eff}. These experimental results of the criticality determination are given in Table I along with the calculated results of k_{eff}.

For the critical configuration of each assembly k_{eff} was calculated with a two-dimensional diffusion theory program (DIXY program of Karlsruhe) in RZ-geometry using both of the 26-group cross section sets, MOXTOT and KFKINR. In these two-dimensional calculations the uranium filled control rods were homogenized for SNEAK-7B over the whole core and for SNEAK-7A over an outer ring of the core, that is, from r_i = 15.86 cm to r_o = 28.63 cm. The results of these calculations are given in the first line of Table I and are taken to represent the basic calculation of k_{eff} to which the various corrections are added.

The corrections calculated for the basic homogeneous calculation were the following:

Table I   Critical Experiment Evaluation

Assembly	SNEAK-7A		SNEAK-7B	
Cross Section Set	MOXTOT	KFKINR	MOXTOT	KFKINR
k_{eff} - 2-Dim.Diffusion (RZ)	.9890	1.0034	.9839	1.0070
$\Delta k_{CYL.}$	-.0045	-.0045	-.0029	-.0029
$\Delta k_{Uran\ rods}$	-.0006	-.0006	.0	.0
$\Delta k_{hetero.}$	+.0006	+.0006	+.0008	+.0008
Δk_{REMO}	+.0015	+.0002	+.0013	-.0010
$\Delta k_{trans.}$	+.0129	+.0129	+.0049	+.0049
k_{eff} =	.9989	1.0120	.9880	1.0088
k_{eff} (experimental)	1.0010		1.0016	

a) <u>Control rod homogenization</u> - The effect of the control rod homogenization was corrected for by using the two-dimensional diffusion theory program in XY-geometry, first with the control rods smeared over the core, as in the RZ-geometry calculation, and second with the control rods represented in their respective positions.

b) <u>Cylindrization correction</u> - A correction for cylindrization was found by comparing a one-dimensional cylindrical diffusion calculation with a two-dimensional diffusion calculation in XY-geometry. In both calculations identical axial bucklings were used.

c) <u>Heterogeneity</u> - The heterogeneity effect of the cell structure was calculated with the program KAPER /4/. The effect was taken as the difference of two KAPER calculations. In one calculation the cell structure was represented as it actually was and in the second as a quasi-homogeneous cell in which the cell thickness was reduced by a factor of 1000.

d) <u>Transport correction</u> - The transport correction was calculated in one dimension with the transport program DTK in S_6. The effect was calculated separately in the axial and radial directions, and then added together unweighted. This procedure was checked in one case by calculating the transport effect with a two-dimensional transport theory program in RZ-geometry to order S_6. The difference between the transport correction calculated in one and two dimensions was slightly less than 1%.

e) Elastic removal correction (REMO) - The REMO correction is
    designed to correct the elastic removal cross sections with
    the weighting spectrum of the composition under investiga-
    tion.

Of the five corrections above only the REMO correction was calculated
with the two cross section sets, MOXTOT and KFKINR. The other correc-
tions were calculated only with the MOXTOT set and assumed to be in-
dependent of the cross section data.

Adding the corrections for the final k_{eff} of the assemblies one
finds that for both assemblies the MOXTOT set underestimates k_{eff}
while the KFKINR set overestimates k_{eff}. However, the k_{eff}'s of
the KFKINR set are more consistent than those of the MOXTOT set
for the two assemblies.

5. Material Buckling Measurements

Unlike the critical mass of an assembly, which depends on the physi-
cal properties and geometry of the core and reflector, the material
buckling of the core is a characteristic parameter of only the com-
position. Mathematically, the material buckling is the eigenvalue
of the space independent multigroup equation, and can be obtained
by the most accurate calculational methods. Therefore, it is a
parameter which is much more suitable for cross section testing
than the critical mass, provided that it can be accurately deter-
mined by experiment.

Method

The method employed at Karlsruhe for the determination of the ab-
solute material buckling was first utilized in fast reactors by
the MASURCA-group in Cadarache, as described by Barberger et al. /8/.
In principle, to obtain the material buckling one must measure the
spatial distribution of the fundamental mode neutron spectrum. In
practice, however, this is not possible. Instead, one is able to
measure the spatial neutron reaction rate distribution with a de-
tector having a microscopic effective cross section $\sigma(E)$,

$$R(\bar{r}) = \int_E \sigma(E)\Phi(\bar{r},E)dE \qquad (1)$$

where the flux distribution, $\Phi(\bar{r},E)$, includes all higher modes
that may exist as a result of the influence of the outer core
zones or reflector. If, however, one possessed a detector having
an effective cross section

$$\sigma(E) = D(E)\Phi^+(E), \qquad (2)$$

where $D(E)$ is the diffusion coefficient and $\Phi^+(E)$ is the fundamen-
tal mode adjoint flux, one could measure directly the curvature of
the fundamental mode spectrum. This is easy to prove if one con-
siders that the function of Eq. (2) filters out the higher modes
of the flux distribution, $\Phi(\bar{r},E)$, in Eq. (1).

However, a detector with an effective cross section of Eq. (2) does
not exist. It is necessary, therefore, to correlate several measured
traverses with linearly independent $\sigma(E)$'s with calculated ones to
synthesize an "experimental" traverse of a detector with the desired

cross section of Eq. (2). The procedure to combine the traverses of these different detectors is accomplished at Karlsruhe in the following manner: Fission rate traverses in the core are measured with four different detectors, two with thermally fissionable isotopes, ^{235}U and ^{239}Pu, and two with fission threshold isotopes, ^{238}U and ^{237}Np. These four measured traverses are fitted by a polynomial. These four traverses, as well as the hypothetical detector with a $D\Phi^+$ cross section, are also calculated with, for example, a two-dimensional diffusion theory program.

At suitable points along the axis of the core the results of the measured traverses are plotted against the corresponding calculated ones, as illustrated in Fig. 1. A least-square fit of a straight line is made to the four resulting points. From the point of the calculated $D\Phi^+$ detector one obtains the "experimental" $D\Phi^+$ point. A repeat of this procedure along the axis of the core yields the "experimental" $D\Phi^+$ traverse from which the experimental material buckling is determined by a least-square fit to a cosine function.

For a cylindrical core the measurements are performed along the axial and radial directions to obtain the total buckling.

Results and Discussion

The results of these measurements in both assemblies are given in Table II. The rather large uncertainty for SNEAK-7A is from the radial buckling. Because of the flux perturbation caused by the control rods, only a small inner portion of the radial traverse could be used for the buckling evaluation, leading therefore to poor accuracy. The calculated material buckling is from a zero-
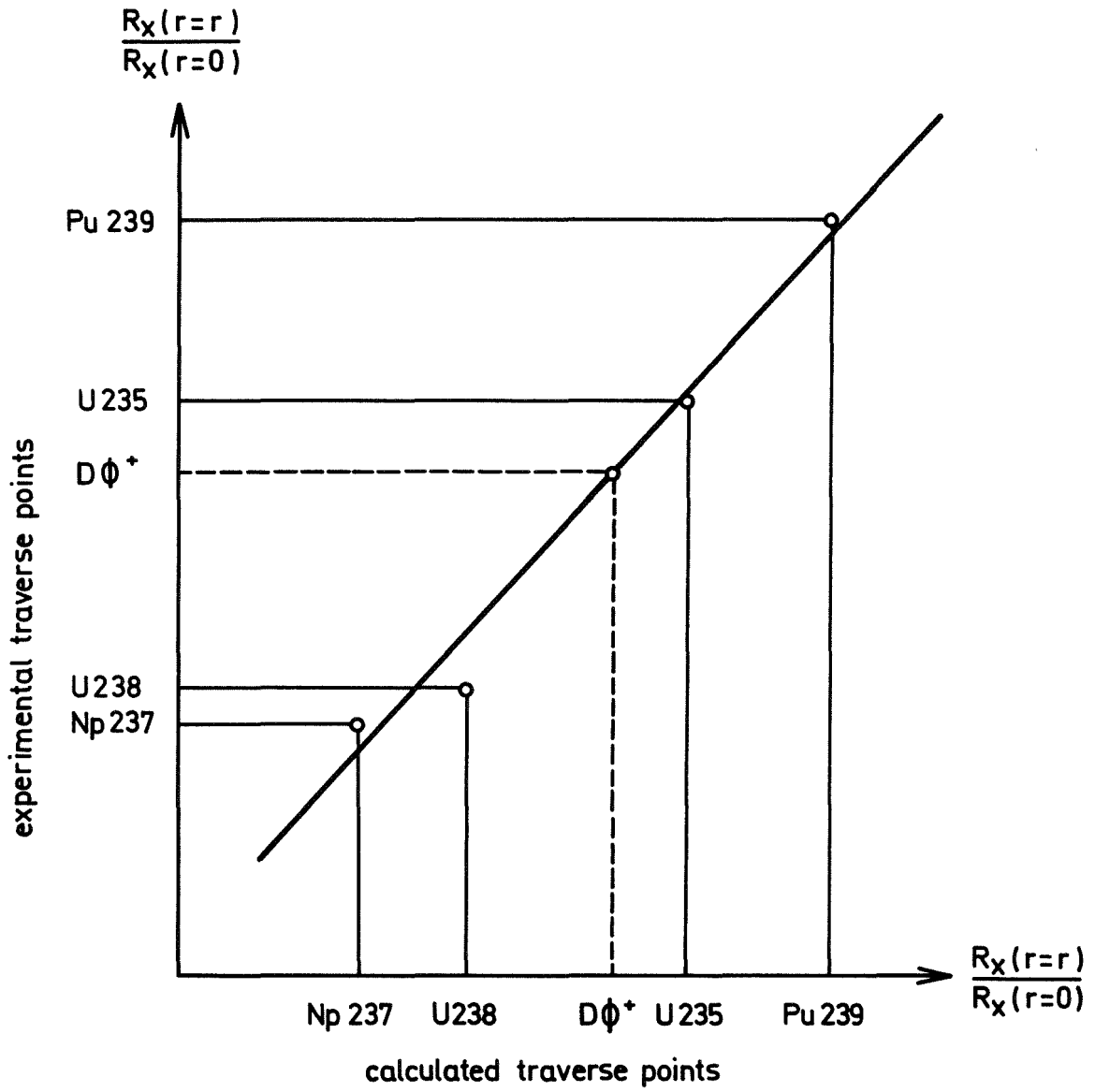
Fig.1   Determination of the "experimental" traverse
         of a DΦ⁺ detector

Table II   Material Buckling and Fundamental Mode Results

	B^2, cm^{-2}	Fundamental mode k_{eff} (B^2_{exp})
SNEAK-7A		
Experiment	$(59.82 \pm .4) \times 10^{-4}$	1.000
MOXTOT	62.06×10^{-4}	1.016
KFKINR	62.91×10^{-4}	1.021
SNEAK-7B		
Experiment	$(34.83 \pm .07) \times 10^{-4}$	1.000
MOXTOT	35.04×10^{-4}	1.002
KFKINR	37.22×10^{-4}	1.018

dimensional homogeneous multigroup calculation. In these calculations the material buckling was the eigenvalue of the equation with k_{eff} set equal to 1.0 minus the corrections for heterogeneity and REMO of the respective assemblies and cross section sets. In all cases the experimental material buckling is overestimated by the calculations. The overestimation ranges from about 1% to 7% depending on the cross section set used and the assembly.

Using the experimentally determined buckling, the fundamental mode k_{eff} was calculated with the zero-dimensional multigroup program. These results are given in the second column of Table II. As in the evaluation of the complete assembly the KFKINR set gives more consistent k_{eff} than the MOXTOT set. In addition, the k_{eff}'s of the fundamental modes are higher than those of the complete assemblies as given in Table I. This result stated in terms of the reflector savings, λ_r, means that the measured λ_r is larger than the calcu-

lated one (see the section on Reaction Rate Traverses in the Appendix A3). It further indicates that in the analysis of earlier critical assemblies, an error in the calculation of λ_r was interpreted as an error in the cross sections of the core material.

6. Spectral Indices

Method

The fission spectral indices, σ_{f8}/σ_{f5} and σ_{f9}/σ_{f5}, were measured with activation foils at the core center. The measurements were normalized to foils irradiated between calibrated parallel plate fission chambers located off-center. The effective mass of the ^{239}Pu-fission chamber relative to the ^{235}U-chamber was determined from the counting rates in a thermal neutron field. The thermal cross section fission ratio, $\sigma_{f9}/\sigma_{f5} = 1.385$, was assumed to be accurate to within $\pm$ 1%, including small corrections for epithermal neutrons. The ^{238}U-fission chamber was calibrated by combined fast and thermal-flux fission rate measurements with a ^{235}U-chamber and a natural uranium chamber.

The spectral indices σ_{c8}/σ_{f5} and σ_{c8}/σ_{f9} were determined from absolute reaction rate measurements. The absolute ^{238}U capture rate was measured with foils. The γ-activity of the 270 keV line was measured with a Ge(Li)-detector, which was calibrated using an ^{243}Am foil of known intensity /9/. For the absolute fission rate determination the effective fissile mass of a ^{235}U-chamber was determined by H. Meister and D. Kuhn using exact chemical

weighing procedures and cross-calibrations to ^{233}U-chambers which were calibrated by low-geometry α-counting. With the effective fissile mass of the ^{235}U-chamber the masses of the ^{239}Pu and ^{238}U-chambers were obtained.

The calibrated chambers were compared with a set of chambers used at Cadarache. The fission ratios were in agreement within the error limits. The difference of 3 to 4% in the absolute masses is not significant, because the absolute Cadarache calibration has a fairly large uncertainty.

In SNEAK-7A the foils were placed between the fuel and graphite platelet. The average cell values were obtained by correcting the measurements with the calculated results of the KAPER-program. In SNEAK-7B special half platelets were employed so that the foils could be positioned between the platelets perpendicular to their surfaces. In this manner cell integrated values were measured directly. A noticeable cell fine structure in both assemblies was found only in the ^{238}U fission rate. In SNEAK-7B the fission rate was 3% larger in the PuO_2UO_2 platelet than in the $U_{nat}O_2$ platelet. A KAPER calculation predicted this fine structure to be 3.3%. The reliability of the KAPER-program for the cell fine structure calculations was checked by means of a bunched cell experiment in SNEAK-7A. The calculations tended to overestimate slightly experimental results. The results were, however, within acceptable limits.

Results and Discussion

The results of the spectral index measurements are given in Table III along with the ratio of the calculation to measurement. The KFKINR cross section set gives a significant improvement in the calculated results over those of the MOXTOT set for σ_{f8}/σ_{f5} and σ_{f9}/σ_{f5}. Quoted also are results calculated with the cross section set based on ENDF/B data. Their close agreement with the KFKINR set is quite surprising.

Table III   Spectral Indices and Leakage in SNEAK-7

| | SNEAK-7A | | | | SNEAK-7B | | | |
| | | Calculation/Experiment | | | | Calculation/Experiment | | |
	Experiment	MOXTOT	KFKINR	ENDF/B	Experiment	MOXTOT	KFKINR	ENDF/B
σ_{f8}/σ_{f5}	$0.0449\pm3\%$	0.785	0.900	0.927	$0.0328\pm2\%$	0.818	0.955	0.943
σ_{f9}/σ_{f5}	$0.984\pm3\%$	0.915	0.985	0.989	$0.975\pm2\%$	0.940	1.014	1.015
σ_{c8}/σ_{f5}	$0.138\pm3\%$	0.95	0.985	0.99	$0.132\pm3\%$	0.985	1.025	1.04
Leakage / Fission rate ^{239}Pu	$1.715\pm4\%$	0.90	0.94	0.924	$1.385\pm4\%$	0.82	0.90	0.87

7. Leakage Measurements and Reaction Rate Balance

To check the consistency of the measured spectral indices with-
in their error limits one can establish a neutron balance at the
core center. However, since the leakage plays a dominant role in
the neutron balance in these small cores (approximately 40% in
SNEAK-7A and 30% in SNEAK-7B) it represents the one factor that
could limit the applicability of such a balance. Therefore the
leakage was experimentally determined indirectly through a series
of reactivity worth measurements. These measurements included the
reactivity worth of core material and a Cf-source at the core
center.

Method

The reactivity worth of core material at the core center is related
to the leakage weighted by the adjoint. From first order perturba-
tion theory the core material reactivity worth at the core center,
per unit volume, is given by

$$\rho_c = \frac{(DB^2\phi)\ \phi^+_{RL}}{\beta_{eff}\ \nu\ R_f\ \phi^+_f\ F} \tag{3}$$

where ρ_c = reactivity worth of core material per cm^3 (dollars),

ϕ^+_{RL} = average adjoint of leakage neutrons,

ν = average number of neutrons per fission,

R_f = absolute fission rate per cm^3 of core material,

ϕ_f^+ = average adjoint of a core fission neutron (adjoint source)

and F = normalization integral, normalized to unit fission source and adjoint source at the core center.

The reactivity scale can be determined from a measurement of the apparent reactivity worth of a Cf-source, which is given by

$$\rho_{Cf} = \frac{S_{Cf}\ \phi_{Cf}^+}{\beta_{eff}\ \nu\ R_f\ \phi_f^+\ F} \tag{4}$$

where ρ_{Cf} = reactivity of a Cf-source (in dollars)

S_{Cf} = source strength

ϕ_{Cf}^+ = average adjoint of a Cf-source neutron.

The remaining parameters in Eq. (4) have the same definitions as those in Eq. (3).

Dividing Eq. (3) by Eq. (4) and rearranging the result to have $(DB^2\phi)$ on the right hand side one finds, after normalizing to the absolute ^{239}Pu fission rate in the core material,

$$\frac{(DB^2\phi)}{R_{f9}} = \frac{\rho_c}{(\frac{\rho_{Cf}}{S_{Cf}}) R_{f9}} \; (\frac{\phi^+_{Cf}}{\phi^+_{RL}}) \tag{5}$$

Description of Experiments

The core material reactivity worth was measured by substituting special platelets of reduced average density for the normal platelets that make up the core unit cell. In this manner one eliminates the strong heterogeneity effects that can result when the entire unit cell is removed. The reactivity worth was determined by a calibrated fine control rod.

The apparent reactivity worth of the ^{252}Cf-source was determined by means of a pneumatic pile oscillator. A detailed description of the measurement is given in the following section. The source strength is known to within $\pm$ 1%.

The absolute ^{239}Pu fission rate in the core unit cell was determined as explained in the section on spectral indices.

The adjoint ratio in Eq. (5) must be calculated. In SNEAK-7A
this ratio was calculated to be 1.03 and, in SNEAK-7B, 1.15.

Results and Discussion

The combination of the above measurements, with the calculated
adjoint ratio, yielded the results given in Table III. Both
cross section sets underestimate the experimental results.

To establish the neutron reaction rate balance the quantities
not measureable were taken from a heterogeneous calculation
performed with the KAPER-program. The results of reaction
rate balance are given in Table IV. The uncertainty in the
calculated ν_9 (^{239}Pu average number of neutrons per fission)
and α_9 (^{239}Pu alpha) was estimated to be 1.5% and 15% respec-
tively. The uncertainty in the other calculated quantities
was neglected.

In the balance, there is a deficiency of neutrons which lies
slightly outside the estimated standard deviation in both
assemblies.

Table IV   Reaction Rate Balance in SNEAK-7

		SNEAK-7A	SNEAK-7B
Production			
ν_9	(b)	2.974 ± 0.045	2.962 ± 0.045
$\nu_8\ R_{f8}/R_{f9}$	(a)	0.391 ± 0.012	0.708 ± 0.014
$\nu_5\ R_{f5}/R_{f9}$	(a)	0.054 ± 0.001	0.136 ± 0.003
$(\nu_{40}\ R_{f40} + \nu_{41}\ R_{f41})/R_{f9}$	(b)	$\underline{0.112}$	$\underline{0.101}$
		3.531 ± 0.046	3.907 ± 0.047
Losses			
$1 + \alpha_9$	(b)	1.235 ± 0.030	1.204 ± 0.030
R_{f8}/R_{f9}	(a)	0.138 ± 0.004	0.249 ± 0.005
R_{c8}/R_{f9}	(a)	0.423 ± 0.013	1.000 ± 0.030
R_{a5}/R_{f9}	(a+b)	0.028	0.069
$(R_{a40} + R_{a41})/R_{f9}$	(b)	0.056	0.051
R_{cSt}/R_{f9}	(b)	0.042	0.064
$- R_{n,2n}/R_{f9}$	(b)	-0.007	-0.008
$(DB^2\phi)/R_{f9}$	(a)	1.715 ± 0.070	1.385 ± 0.055
		3.630 ± 0.077	4.014 ± 0.070
Production - Losses		-0.099 ± 0.090	-0.107 ± 0.084

(a) Experimental value

(b) Calculated value with the KFKINR cross section set

8. Neutron Importance

The experimental determination of the energy dependence of the
neutron importance function is of value as a further check in
the search for resolving discrepancies involved in the inter-
pretation of fast critical assembly measurements. For example,
the correct prediction of the sodium void reactivity effect
depends upon, among other things, how well the importance func-
tion is defined in energy. It also plays a very important role
in small-sample reactivity worths.

Description of the Measurement (SNEAK-7B)

To measure the energy dependence of the importance function seven
different neutron sources were oscillated between the core center
and a position outside of the core with a pneumatic pile oscil-
lator /10/. The reactivity effect of the source was determined by
compensation with a calibrated automatic control rod. The reac-
tivity effect of the source consists of two components. One com-
ponent is the desired apparent reactivity of the source neutrons
which is inversely proportional to the flux level. The second
component, which must be corrected for, is due to the absorption
of neutrons in the source itself and its capsule. The effect of
the source neutrons can be extracted from two measurements, one
at low power ($\sim$ 0.3 watts) where the source effect is dominating,
and one at higher power ($\sim$ 30. watts) where one measures essen-
tially the effect due to absorption.

The effective source strength obtained is expressed as

$$Q_s^i = \int \phi^+(E) S_i(E) dE \qquad (6)$$

where $S_i(E)$ is the source neutron spectrum of the ith source.

In order to cover the energy range below 20 keV water moderated
Pu/Li and Sb/Be sources were used. Instead of oscillating these
sources, water was pumped back and forth between the source and
a dummy source so that the moderation effect of the water could
be obtained. The neutron spectrum of the moderated sources were
determined from a one-dimensional S_n-transport calculation of
order S_8.

Results and Discussion

The results of these measurements are given in Table V. For com-
parison with calculations the experimental results are normalized
to the Cf-source and one source neutron. The source strength of
the various sources was determined by the Manganese bath method
to an accuracy of about 1%.

The calculated results in Table V were obtained by folding the
known neutron source spectra with the importance step-function
from 26-group calculations, and applying a correction which
approximately takes into account the real shape of the impor-
tance function (above 1 keV), as obtained from a 208-group cal-
culation. This procedure also corrects largely for the error
that is introduced by using flux-weighted group cross sections
for the calculation of the 26-group importance function. This
correction amounts to a maximum of 1.2%.

Table V   Integral Importance of Various Neutron Sources in SNEAK-7B

Neutron Source	Mean Energy (MeV)	Source Worth[+]		
		Experiment	Calculation (MOXTOT)	Calculation (KFKINR)
Pu/C13	5.1	1.18 ±0.015	1.155	1.16
Am/Be	5.0	1.147±0.015	1.13	1.135
Am/B11	2.9	1.074±0.01	1.073	1.075
Cf-252	2.3	1.000±0.01	1.000	1.000
Pu/F	1.4	0.918±0.01	0.928	0.925
Pu/Li7	0.45	0.85 ±0.008	0.853	0.845
Pu/Li7^{mod}	0.3	0.85 ±0.01	0.866	0.85
Sb/Be	0.039	0.712±0.007	0.75	0.715
Sb/Be^{mod}	0.017	0.80 ±0.01	0.885	0.85

[+] Source worth per unit source strength, normalized to ^{252}Cf-source

The error of the measured quantities is computed from the statistical error in the reactivity determination and the error in the relative source strengths.
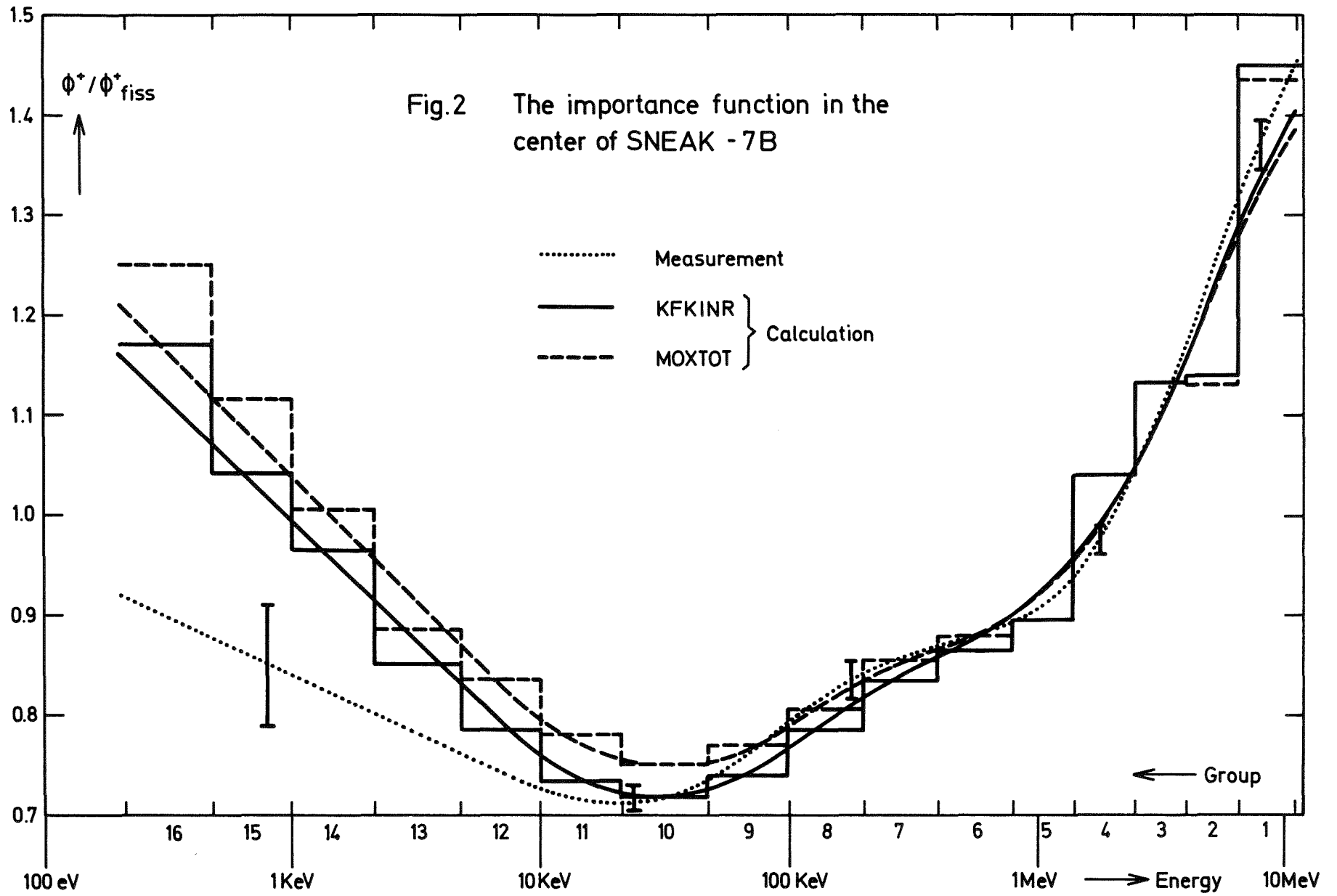
The calculated source worths have an error of 0.5 to 1.0% due to the uncertainty in the neutron source spectra.

By unfolding the integral experimental worths Q_s^i of Eq. (6) with the methods of Ref. /10/ the energy dependence of the importance function in the center of SNEAK-7B was obtained. The results are shown in Fig. 2 together with the results of the 26-group calculations, as well as the two functions which are found by unfolding the calculated integral values given in Table V. In this manner easy comparison of experimental and theoretical results is possible. All these functions are normalized to give 1 for the integral importance of a unit strength fission source.

It should be noticed that in the low energy region below 20 keV, the unfolding results are determined essentially by only one integral value (Sb/Be^{mod}), so that the shape of the importance function may be very different in reality. The relatively large error in this energy region is mainly due to the fact that the Sb/Be^{mod} source emits a substantial number of neutrons below 200 eV (about 13%). In order to perform the unfolding above 200 eV, one has to correct for the neutrons below 200 eV with a calculated importance function. Assuming an error of 10% for this correction and a realistic uncertainty in the calculated moderated spectrum, one finds the shown error margins for the unfolded result in the low energy region.

Significant discrepancies between experiment and calculation exist only for the Sb/Be and Sb/Be^{mod} sources, where the experimental values are about 5% and 10% below the MOXTOT calculated values. The respective KFKINR values agree substantially better, but the measured Sb/Be^{mod} value is still 6% below the calculation.

Fig. 2 shows what these differences mean for the energy dependence of the importance function.

Fig.2   The importance function in the center of SNEAK - 7B

.... Measurement

———— KFKINR ⎫
                ⎬ Calculation
- - - - MOXTOT ⎭

ϕ^+/ϕ^+_{fiss}

← Group

→ Energy

100 eV   1 KeV   10 KeV   100 KeV   1 MeV   10 MeV

- 25 -

- 26 -

9. Central Reactivity Worths

Of the measurements performed in Pu-fueled fast critical assem-
blies, the central reactivity worths of fissionable materials
have been, typically, the most difficult to reproduce by calcu-
lation. In some cases the overestimation of the worths by cal-
culation has been as great as 30%. Improved cross section data
and more sophisticated calculational methods available at Karls-
ruhe offered some hope for improvements in this area. Therefore,
these measurements were included in the investigations on the
SNEAK-7 assemblies.

Description of the Experiment

The central reactivity worths of several important isotopes were
measured with a pneumatic pile oscillator at the core center in
both assemblies. The samples had a cross section of 4.6×4.6 cm^2
and thicknesses ranging from 0.157 to 0.628 cm. The oscillator
element was filled so that the regular core lattice was not
disturbed at both end positions of the oscillator stroke. In
SNEAK-7A the reactivity effect of the sample movement in the
oscillator was determined from the flux signals by the inverse
kinetics method with corrections applied for the transport of
neutron precursors. For comparative purposes and reliability
checks some measurements were repeated using a calibrated auto-
matic control rod. In SNEAK-7B most of the measurements were
performed utilizing the calibrated automatic control rod.

Results and Discussions

The reactivity worth calculations were performed with the KAPER-program which accounts for the heterogeneity of the sample and its environment. The program utilizes exact perturbation theory, with the perturbed flux for the sample and its surroundings, to calculate the worths. Significant improvements over the results of a first-order diffusion theory perturbation calculation are found with this program, particularly for the ^{238}U, ^{10}B and Ta samples.

The normalization integrals for the two assemblies were taken from a two-dimensional homogeneous diffusion theory calculation in RZ-geometry. The values of β_{eff}, which were used to convert the calculated reactivities to dollars, were also obtained from these two-dimensional calculations with the β values from Keepin /11/. The values were the following:

$$\beta_{eff}$$

Cross section set	SNEAK-7A	SNEAK-7B
MOXTOT	0.00348	0.00396
KFKINR	0.00359	0.00400

The results of the reactivity worth measurements and calculations are given in Table VI. Also given is the reactivity effect of a ^{252}Cf-source normalized to the total fission rate in the core unit cell. The differences of the homogeneous and heterogeneous calculations are shown separately for each sample in the columns marked "(Hom.-Het.)/Hom.". The worths quoted as the ratio of calculation to experiment are from the heterogeneous calculation.

Table VI   Material Worths at the Core Center, 10^{-3} $/g

Sample	Sample weight (gm)	SNEAK-7A				SNEAK-7B			
		Experiment	Calc./Exp.		Hom-Het/Hom (%)	Experiment	Calc./Exp.		Hom-Het/Hom (%)
			MOXTOT	KFKINR			MOXTOT	KFKINR	
^{235}U	3.7	2.25±3%	1.213	1.082	2.38	1.265±2%	1.185	1.082	-0.8
^{238}U	124	-0.110±3%	1.385	1.078	7.23	-0.0670±2%	1.330	1.100	4.0
^{239}Pu	2.5 (7A) 4.0 (7B)	3.03±3%	1.150	1.085	2.69	1.695±2%	1.082	1.062	-0.54
^{240}Pu	3	0.72±8%	0.81	0.99	5.15	0.30±10%	0.83	1.06	2.12
^{10}B	0.3	-55.2±2%	1.283	1.045	6.49	-20.7±2%	1.190	1.005	5.09
Ta	36	-0.865±2%	1.34	1.082	30.7	-0.320±2%	1.31	1.132	20.1
Eu_2O_3	3.6	-3.49±2%	1.04	--	4.08	-1.17±3%	1.11	--	2.23
Fe	25 (7A) 51 (7B)	-0.096±15%	1.06	0.995	1.79	-0.060±5%	1.09	1.135	2.16
SS	27 (7A) 54.6 (7B)	-0.082±15%	1.28	1.254	4.34	-0.060±5%	1.20	1.254	0.3
Cf-source (1/βνF)	10^{-3} $/cm^3	2.04±4%	1.25	1.16	--	0.84±4%	1.18	1.14	--

As normally observed in Pu-fueled fast critical assemblies, the calculations significantly overestimate the worths. The consistency of the results are improved greatly with the KFKINR cross section set. Since the KFKINR set gives a slightly harder spectrum than the MOXTOT set, the fission portion of the reactivity effect (positive) of ^{238}U and ^{240}Pu is increased giving better calculated results. The KFKINR set yields also a larger normalization integral and larger β_{eff}'s since this cross section set calculates the fission contribution of the isotopes better (see Table III. Spectral Indices). In spite of this the worths are still overestimated with the KFKINR set by approximately 8% which is due, in our estimation, primarily to low delayed neutron data.

10. Zero Power Transfer Function

The experimental determination of reactivity worths by oscillator experiments usually makes use of the inverse kinetics method and depends, therefore, on the delayed neutron data used in the inverse kinetics program. An important check on these data can be provided by a measurement of the reactor transfer function.

The zero power transfer function is defined as the ratio of the flux amplitude and the reactivity amplitude of a harmonic oscillation. It is related to the delayed neutron parameters by the equation

$$\frac{\delta n / n}{\delta k / \beta} = \frac{1}{\omega \left[\frac{1}{\beta} + \sum_i \frac{a_i}{\lambda_i + \omega} \right]}$$

Description of Measurement

A measurement of the transfer function was performed in SNEAK-7B by oscillating a calibrated fine control rod at different frequencies. The worth of the control rod was about 2 ¢. The Fourier coefficients of the fundamental frequency of the flux and reactivity signal were determined. They provide immediately the amplitude and the phase of the transfer function.

No systematic algorithm for drift correction was applied. However, it was observed that the influence of the drift can be minimized in the following way. The Fourier coefficient δn_1 of the flux signal $\delta n(t)$ is given by

$$\delta n_1 \cos \phi = \frac{1}{T} \int_0^T \delta n(t-t_0) \cos \omega t \, dt$$

$$\delta n_1 \sin \phi = \frac{1}{T} \int_0^{To} \delta n(t-t_0) \sin \omega t \, dt$$

where the phase angle ϕ depends on the starting time t_0 of the integration. It was found that the influence of the drift on $|\delta n_1|$ is minimized if t_0 was selected such that $\phi = 0$, whereas the influence on the phase angle of the transfer function is minimized if $\phi = 90^\circ$. Thus, two separate evaluations for the amplitude and the phase were carried out.

Results and Discussions

The results are shown in Figs. 3 and 4 together with the calculated values obtained with delayed neutron data from the KFKINR set. In
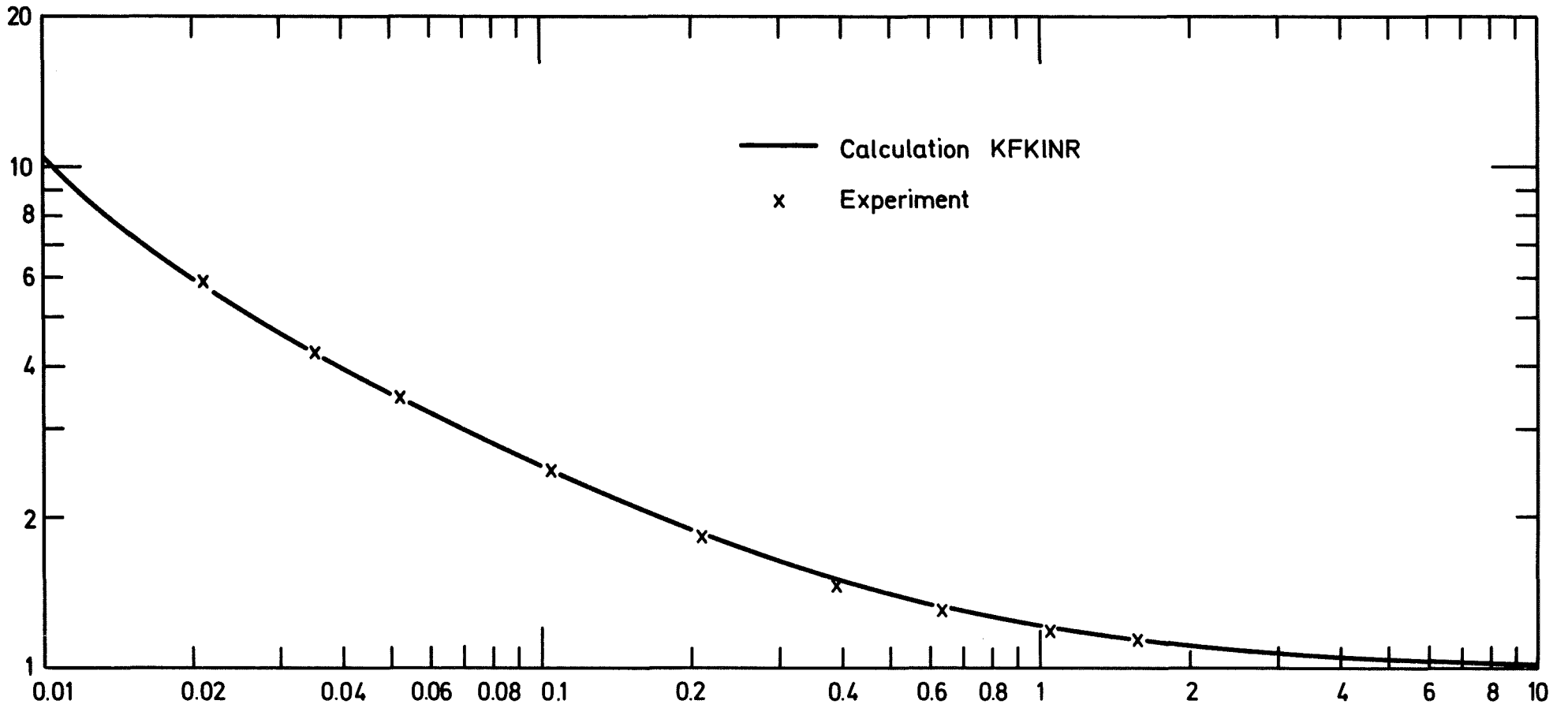
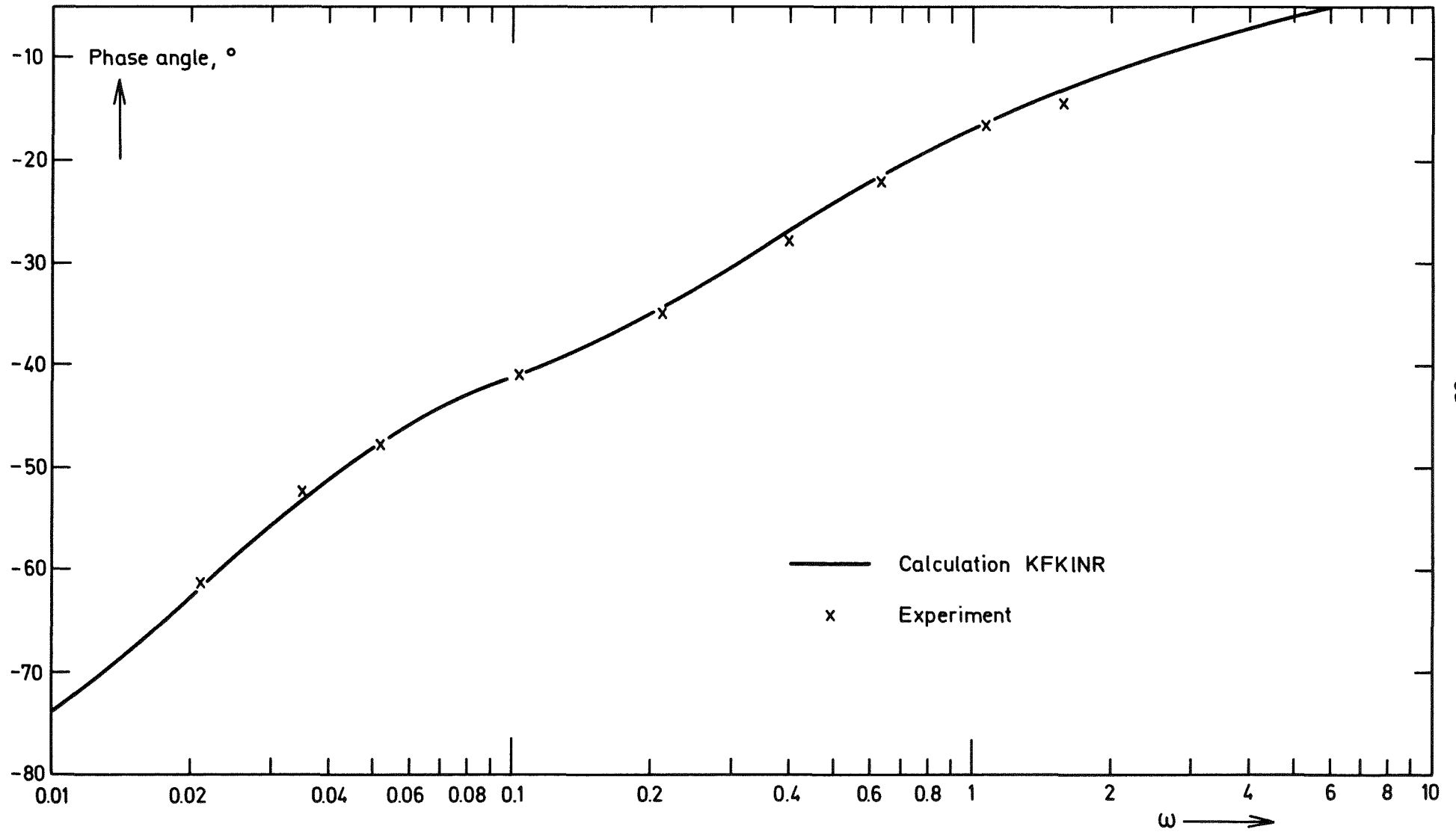Fig.3   Amplitude of the transfer function , SNEAK - 7B

Fig.4   Phase of the transfer function , SNEAK-7B

order to eliminate errors in the rod calibration, the measured
amplitudes were normalized to the calculation at the highest
frequency. The agreement with calculation is good.

The calculated transfer function is rather insensitive to changes
in the delayed neutron data, and any difference between measure-
ment and calculation could only be explained by rather large
changes in the data. However, the results lead to the conclusion
that one understands the behaviour of the transfer function in a
fast plutonium core.

11. Measurements of β_{eff} and Normalization Integral

As mentioned in a previous section a discrepancy which has been
observed for several years in the analysis of Pu-fueled fast
critical experiments is an overestimation of central reactivity
worths by calculation. From the results in Section 9. (Table VI)
one sees that the overestimation depends on the cross section
set. Nevertheless the overestimation appears to be larger in Pu
assemblies than in similar uranium fueled assemblies. This dis-
crepancy puts a rather large uncertainty on the reactivity scale
of projected fast breeder reactors, and limits the use of results
obtained in zoned critical assemblies in fast breeders. Further-
more, there is no obvious explanation for this discrepancy since
both the experimental technique and the calculational model are
considered adequate. Therefore, it seems that the discrepancy
could be caused either by incorrect cross section data, or by
incorrect delayed neutron data. In terms of integral quantities,
the question would be whether there is an error in β_{eff}, in the

normalization integral, or in the cross sections of the specific
isotopes under study. The observation that ratios of reactivity
worths are usually predicted much better than their absolute val-
ues seems to exclude the latter possibility.

In view of the interest this problem has in fast reactor physics,
a systematic study to determine β_{eff} and the normalization inte-
gral was carried out in the two assemblies, SNEAK-7A and 7B. Three
types of measurements were performed in these assemblies. In the
first, β_{eff} and the normalization integral were determined by a
set of measurements involving the apparent reactivity worth of a
^{252}Cf-source. In the second measurement, ratios of β_{eff}'s of dif-
ferent fuel isotopes were obtained by measuring the effect due to
the transport of precursors in the pile oscillator. The third
measurement of β_{eff} was performed by a frequency analysis of
the reactor noise.

11.1.   Measurement of β_{eff} with a ^{252}Cf-source

Method

The effective delayed neutron fraction β_{eff} of a fast critical
assembly can be measured by a technique which uses a ^{252}Cf-source
of known source strength. Perturbation theory gives the following
expression for the apparent reactivity of a ^{252}Cf-source placed
at the center of a reactor

$$\rho_{Cf} = \frac{S_{Cf} \, \phi^+_{Cf}}{\beta_{eff} \, \nu \, R_f \, \phi^+_f \, F} \qquad (7)$$

Eq. (7) is a repeat of Eq. (4) in Section 7. and has, therefore, the same notation definition.

The normalization integral F, which is normalized to unit fission source S_f and adjoint source at the core center, is given by

$$F = \frac{\int d^3r \; S_f(r)\Phi_f^+(r)}{S_f(o)\Phi_f^+(o)} \tag{8}$$

The technique consists of measuring ρ_{Cf} and the absolute fission rate R_f at the core center. Both measurements must be normalized to the same reactor power. The correction factor Φ_{Cf}^+/Φ_f^+ for the small difference in the adjoint between core fission neutrons and ^{252}Cf-neutrons must be calculated.

According to Eq. (7), one obtains the product $\beta_{eff}\nu F$ from these measurements. In order to determine the normalization integral, measured axial and radial traverses of fission rates, and of the ^{252}Cf worth are used. ν can be calculated with good accuracy from basic data. Combining these results, an experimental value of β_{eff} is obtained.

Description of the Experiments

A ^{252}Cf spontaneous fission source, which was calibrated at Saclay by the Manganese bath technique, was used in the experiment. The source strength is known with an error of about 1%, which includes both statistical and possible systematic errors. The measurements were carried out with the pile oscillator, using a calibrated auto-

matic control rod. The apparent reactivity of the source neutrons was determined through two measurements in a manner explained in Section 8. The results of the measurements are given in Table VII. Also given is the current from a BF_3 chamber, positioned in the blanket, which was used to define the flux level for the experiment.

The absolute fission rates were measured with activation foils of ^{239}Pu and ^{238}U. The foil measurements were normalized to absolutely calibrated parallel plate fission chambers. Some details on the calibration and on the experiment are given in Section 6. The absolute fission rate measurements gave, relative to the BF_3 chamber current, 3.40×10^{13} fissions/cm^3 Amp in 7A and 1.435×10^{13} fissions/cm^3 Amp in 7B.

The measured fission chamber traverses, and the ^{252}Cf worth traverses were used to obtain an experimental normalization integral. Polynomial fits were obtained for the experimental and measured traverses, both in axial and radial direction. From these fits, correction factors between the experimental and calculated normalization integral were derived. It is assumed implicitly in this procedure that the flux in separable in RZ-geometry, or rather that the deviation from separable fluxes is correctly calculated. The measurement of an axial fission traverse in a sub-assembly near the boundary (Appendix A1) indicates that this assumption is valid. The error on the experimental normalization integral was estimated to about 2%.

Results and Discussion

The results of these experiments are given in Table VIII. Also shown are results of standard calculations with two-dimensional diffusion

Table VII   Results of ^{252}Cf Measurements

Assembly	Date of experiment	Source strength 10^6 n/sec	Measured reactivity worth of source neutrons, $\cancel{c}$	Current of BF_3 chamber 10^{-8} Amp	Calculated ratio Φ^+_{Cf} / Φ^+_f
7A	21.12.70	1.117±1%	1.993±1%	0.353	1.005
7B	23. 6.71	0.978±1%	1.438±1%	0.400	1.005

Table VIII Results of β_{eff} Measurements with a ^{252}Cf-Source

	$\beta\nu F$, cm^3	F, cm^3	ν	β_{eff}	σ_{f8}/σ_{f9}	σ_{f5}/σ_{f9}
SNEAK-7A						
Experiment	491±4%	40000±2%		0.00416±5%	0.0456±3%	1.016±3%
Stand. Calc. MOXTOT	394	38500	2.95	0.00347	0.0391	1.110
Stand. Calc. KFKINR	424	40000	2.95	0.00359	0.0416	1.030
SNEAK-7B						
Experiment	1195±4%	92000±2%		0.00446±5%	0.0336±3%	1.026±2%
Stand. Calc. MOXTOT	1010	87400	2.92	0.00396	0.0293	1.092
Stand. Calc. KFKINR	1048	90000	2.92	0.00400	0.0317	1.010

theory, where the MOXTOT and KFKINR set were used. For the
standard calculation of β_{eff} the values $\beta_5 = 0.00641$, $\beta_8 =$
0.0148, $\beta_9 = 0.00204$, $\beta_{40} = 0.00266$, which were obtained from
Keepin's data for fast fission /11/, were used. The fission
ratios are also given. The following conclusions can be drawn
from a comparison of the measured and calculated values.

a) The normalization integral is underestimated by the
MOXTOT set, but calculated fairly well with the im-
proved cross section set KFKINR. There is no signifi-
cant difference between the results for the two assem-
blies.

b) β_{eff} is strongly underestimated by the MOXTOT set, the
difference being 17% for 7A, and 11% for 7B. With the
KFKINR set, the underestimation is reduced somewhat,
but it is still present. It must be pointed out that
in a core fueled with $PuO_2{}^{238}UO_2$ the contributions of
^{239}Pu and ^{238}U to β_{eff} are of comparable magnitude.
Therefore, one expects that the β values calculated
with different cross section sets are correlated with
the calculated fission ratio σ_{f8}/σ_{f9}.

The KFKINR set calculates the fission ratio much better than
the MOXTOT set, but still largely underestimates β_{eff}. In
fact, it calculated β_{eff} only slightly better than the MOXTOT
set. Therefore, it must be assumed that this underestimation
is caused by incorrect delayed neutron data.

11.2. Measurement of β_{eff} Ratios with a Pile Oscillator

Description of the Experiment

In SNEAK-7B, an experiment was carried out in which a subassembly, uniformly loaded over its full length, was oscillated with a pneumatic pile oscillator. The pseudo reactivity effect observed in this experiment is due to the transport of delayed neutron precursors. In order to compare the effect of precursors of different isotopes, four different loadings of the oscillated subassembly were used. The atom densities are given in Table IX. The loading Pu1 was essentially the core loading at a reduced fuel density. In the loading U1, Pu was replaced by ^{235}U. The loadings Pu2 and U2 had the same fissile content as Pu1 and U1, but about half of the ^{238}U is replaced by inert material.

The stroke of the oscillator was 80 cm; the core height was 70 cm. The uranium loadings were completely uniform over a length of 160 cm. However, the Pu loadings, due to shortage of Pu platelets, contained two Pu regions of 70 cm height each, which were separated by a 10 cm region filled with the corresponding uranium composition. This uranium region was moved through the core during the oscillation.

Oscillations with half-periods of 30 sec, 60 sec, and 120 sec were performed. The transit time of the oscillator was about 1.5 sec. Therefore, the experiment gives information only on the effect of the four slow groups of delayed neutrons.

Table IX   Atom Densities of the SNEAK-7B Core and the
Pile Oscillator Loadings (10^{20} atoms/cm^3)

	Core	Pile Oscillator Loadings			
		U1	U2	Pu1	Pu2
^{235}U	1.063	19.258	18.792	0.709	0.290
^{238}U	145.68	107.11	49.16	97.36	39.40
^{239}Pu	19.741	--	--	13.088	13.055
^{240}Pu + ^{242}Pu	1.781	--	--	1.181	1.178
^{241}Pu	0.161	--	--	0.107	0.107
Al	0.12	100.46	134.27	34.21	68.20
C	0.66	0.26	130.95	0.43	131.18
Cr + Mn	29.25	29.15	23.36	35.08	29.28
Fe	99.58	98.64	78.09	119.21	98.60
Ni	14.60	15.01	11.97	16.68	13.63
O	338.38	217.00	99.47	225.75	108.14

Theoretical Model and Data Evaluation

The periodic flux oscillations due to the square wave oscillation of a subassembly were studied by Kussmaul and Meister /12/. The flux oscillates in the same manner as if a periodic reactivity were present. This pseudo-reactivity, calculated to first order in the flux amplitude /12/, is given by

$$\rho(t) = - \gamma_1 \sum_i \frac{\beta_i e^{-\lambda_i t}}{1 + e^{-\lambda_i T}} + \gamma_2 \qquad (9)$$

where T is the half period of the pile oscillator, β_i and λ_i are delayed neutron parameters, and the γ's are constants. One can write Eq. (9) for several fuel isotopes, inserting the correct expression for the coefficient γ_1

$$\rho^{(n)}(t) = - \frac{1}{\beta_{eff} NJ} \int_{V_p} d^3 r \phi_d^+(r) \phi(r) \sum_k \beta_k \nu_k N_k^{(n)} \sigma_{fk} \delta_k^{(n)} F_k(t) + \gamma_2 \qquad (10)$$

with the following notation

$\rho(t)$ reactivity in dollars

k   index of the fuel isotope

V_p volume of the pile oscillator inside the core

$\phi(r)$,

$\phi_d^+(r)$ unperturbed neutron flux and adjoint of delayed neutrons in the pile oscillator volume

N_k atom density of isotope k

σ_{fk} spectrum averaged fission cross section for the homogeneous core

NJ   normalization integral

β_{eff} effective delayed neutron fraction of the reactor

The superscript n labels the different loadings of the pile oscillator. $\delta_k^{(n)}$ is a calculated correction factor, close to unity, which relates the microscopic fission rate in the isotope k for the nth loading to the fission rate for the homogeneous core. The function $F_k(t)$ is defined by

$$F_k(t) = \sum_i \frac{a_{ik}\, e^{-\lambda_{ik}t}}{1 + e^{-\lambda_{ik}T}} \qquad (11)$$

where the a_i's are the relative delayed neutron fractions of the isotope k.

Eq. (10) states that, after the movement of the oscillator, a negative reactivity due to the loss of precursors appears, which is, apart from the time factor $F_k(t)$, equal to the relative contribution of the pile oscillator volume to the total β_{eff} of the reactor. This time dependent negative reactivity is compensated by the positive constant reactivity γ_2 to give an average reactivity of zero over one period of the periodic oscillation. Obviously, Eq. (10) may be written as

$$\rho^{(n)}(t) = - \sum_k C_k^{(n)} \beta_k \nu_k \sigma_{fk} \cdot F_k(t) + \gamma_2 \qquad (12)$$

The evaluation of the experiments was done simultaneously for
two loadings which differ by their ^{238}U content. As required
by Eq. (12), the reactivity traces $\rho(t)$ were fitted to sums
of functions $F_k(t)$, where the coefficients, and also the con-
stant reactivity γ_2, were determined by the fit. The func-
tions $F_k(t)$ were calculated using the delayed neutron data
of Keepin /11/. Thus, the experiments with the loadings U1
and U2 determine β_5 and β_8, and the experiments with Pu1 and
Pu2 determine essentially β_8 and β_9, apart from a factor com-
mon to all β's which is proportional to the inverse normaliza-
tion integral.

The transit behaviour of the pile oscillator was described by
a model suggested by Boix-Amat /13/. The assumptions are that
the motion of the pile oscillator is linear, and that both the
flux and adjoint flux have an axial cosine distribution. Typi-
cal runs for the loadings U2 and Pu2 are shown in Fig. 5 and 6.

Results
___

The experiment determines essentially the amplitudes

$$\sum_k C_k^{(n)} \beta_k \nu_k \sigma_{fk}$$
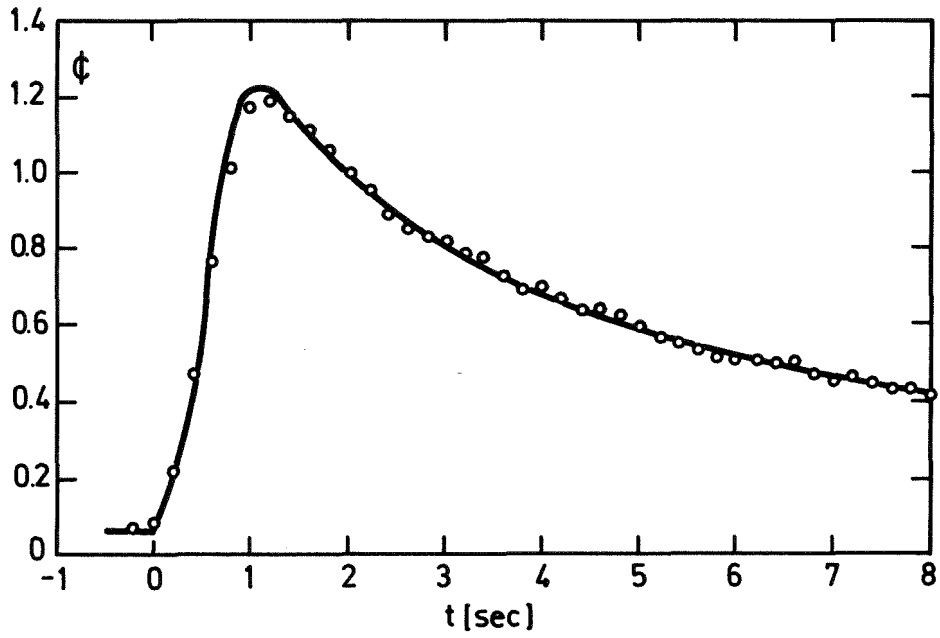
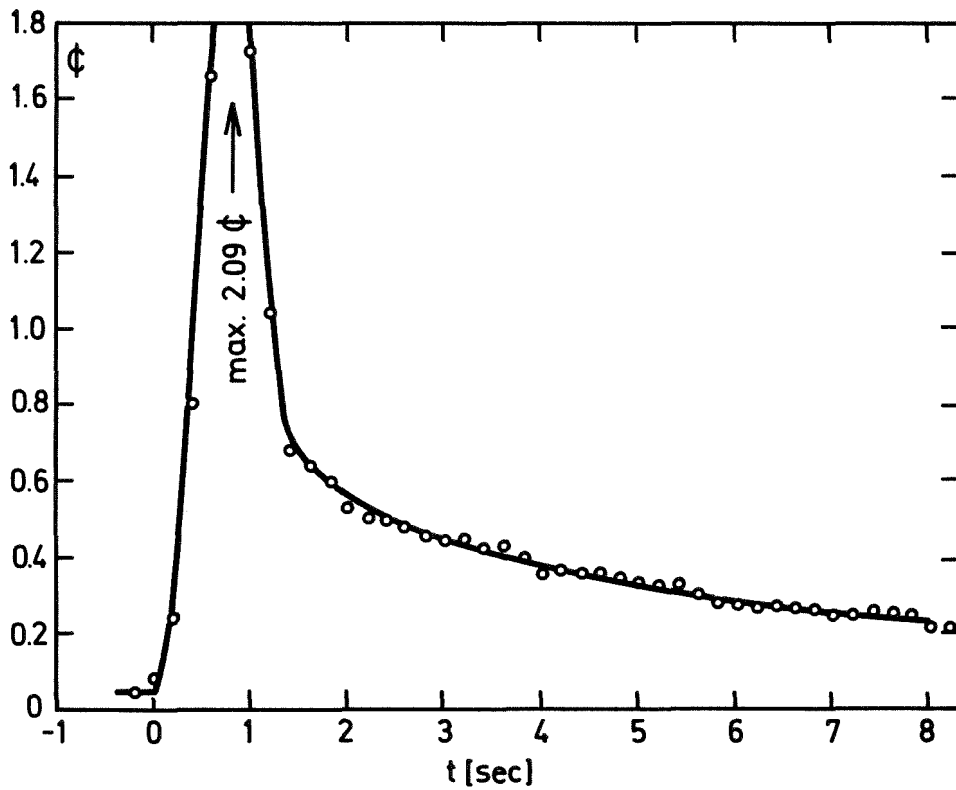Fig.5   Reactivity plot for the loading U1
         T = 60 sec

Fig.6   Reactivity plot for the loading Pu 1
         T = 60 sec

as defined in Eq. (12). The results are given in Table X, along
with calculated values. The KFKINR set was used, and one-dimen-
sional diffusion theory was employed. For the loading Pu1,
which has about the core composition, the amplitude is essen-
tially the inverse normalization integral; it is slightly under-
predicted by the calculation. However, the amplitudes for the
uranium loadings are overpredicted, which indicates an over-
prediction of the ratio β_5 : β_{Pu}. The evaluation for the ratios
$\beta \nu \sigma_f$ gives

$$\frac{\beta_8 \nu_8 \sigma_{f8}}{\beta_5 \nu_5 \sigma_{f5}} = 0.094 \pm 10\%$$

$$\frac{\beta_9 \nu_9 \sigma_{f9}}{\beta_5 \nu_5 \sigma_{f5}} = 0.475 \pm 8\%$$

With the experimental fission ratios in SNEAK-7B, as given in
Table III, one obtains the $\nu\beta$ ratios given in Table XI. Keepin's
values for these ratios are also listed. For better comparison,
the values from this experiment are normalized to Keepin's value
for $\nu\beta_5$, assuming that this value is the best established one.
Then, $\nu\beta_8$ is about 15% larger, and $\nu\beta_9$ is 25% larger than Keepin's
value. However, the errors on these figures are rather large.

Table X   Measured Amplitudes for Different Loadings

	U1	U2	Pu1	Pu2
Amplitude Eq. (12), $ x 10^3				
T = 30 sec	16.54	13.42	9.65	6.16
T = 60 sec	16.78	13.78	9.59	6.27
T = 120 sec	16.96	13.83	9.28	6.44
Mean	16.76±0.2	13.68±0.2	9.52±0.2	6.31±0.2
Calculated (KFKINR)	17.80	14.75	8.90	5.65

Table XI   Experimental Values of ($\nu\beta$) Ratios

	$\dfrac{\nu_8\beta_8}{\nu_5\beta_5}$	$\dfrac{\nu_9\beta_9}{\nu_5\beta_5}$	$\nu_5\beta_5$	$\nu_8\beta_8$	$\nu_9\beta_9$
This experiment	$2.85\pm10\%$	$0.488\pm8\%$	0.0165	$0.0470^{a)}$	$0.00805^{a)}$
Keepin	2.50	0.382	0.0165	0.0412	0.0063

a) Normalized to Keepin's value for ^{235}U

11.3. Measurement of β_{eff} by Noise Analysis

In a zero-power reactor noise experiment, the inherent statistical fluctuations of the neutron population about some average value can be analyzed to determine kinetic parameters of the reactor. These parameters include the prompt neutron decay constant α and the product $\beta_{eff}^2 R_f$, where R_f is the total fission rate in the reactor. Through an independent measurement R_f can be determined, thereby yielding from the noise measurement β_{eff}.

Method

The theory of correlation experiments /14/, under the assumption of the point reactor model, yields through the frequency analysis of two ion-chamber currents the cross-power spectral density as given by

$$CPSD(\omega) \;=\; q_1 q_2 W_1 W_2 R_f \; \frac{Dk^2}{1^2} \; |H(\omega)|^2 \qquad (13)$$

where q_n = average charge per detected neutron in detector n,

W_n = detector sensitivity (counts per fission)

R_f = fission rate in the reactor

$D = \dfrac{\overline{\nu^2} - \overline{\nu}}{\overline{\nu}}$ where $\overline{\nu}$ is the average number, and $\overline{\nu^2}$ the mean square of the number of neutrons per fission

k = effective neutron multiplication constant

l = prompt neutron lifetime

and $H(\omega)$ = zero-power reactor transfer function at frequency ω.

The mean ion-chamber current is

$$I_n = q_n W_n R_f. \tag{14}$$

Considering only the high frequency range where the effect of delayed neutrons can be neglected, one has for the transfer function

$$\left| H(\omega) \right|^2 = \frac{1}{\omega^2 + \alpha^2}$$

with

$$\alpha = \frac{1 - k \left(1 - \beta_{eff} \right)}{l}$$

At delayed critical $k = 1$ and, therefore, $\alpha = \alpha_c = \beta_{eff}/l$. The Eq. (13) can then be written, using also Eq. (14), as

$$CPSD(\omega) = \frac{I_1 I_2}{R_f} \frac{D}{l^2} \frac{1}{\alpha_c^2 + \omega^2}. \tag{15}$$

For the frequency range $o \ll \omega^2 \ll \alpha_c^2$ the ω^2 in the denominator of Eq. (15) can be neglected, yielding

$$\frac{CPSD(\omega)}{I_1 \, I_2} = \frac{D}{\beta_{eff}^2 \, R_f} \qquad (16)$$

With an independent measurement of the total fission rate R_f, β_{eff} can be determined from Eq. (16). D is simply a nuclear parameter which is known to good accuracy.

In the case that the point reactor model, assumed in the derivation of Eq. (13), is not valid one must provide for the space and energy dependence of the neutron flux in the derivation of the correlation function. However, this results in essentially the same equation with a correction factor $g \geq 1.0$ /15/. Therefore

$$\beta_{eff} = \sqrt{\frac{gD}{R_f} \cdot \frac{I_1 \, I_2}{CPSD(\omega)}} \, . \qquad (17)$$

Description of the Experiment

The frequency analysis of the reactor noise was performed with two sets of coupled ^{3}He-detectors operated in the current condition with 400 volt batteries. The detectors were positioned at the core midplane in the core position (17-19) of both the

- 52 -

SNEAK-7A and 7B assemblies (see Figs. Al-1 and Al-3). The fluc-
tuations and the mean value of the ionization chamber currents
were amplified separately. The outputs of two band pass filters,
which filtered the current fluctuations in the desired frequency
range, were multiplied together and integrated. When divided by
the integration time, the band width, and the amplification,this
gave directly the cross-power spectral density.

The measurement of the integrated mean value of the ionization
chamber currents was achieved with an Analog-to-Digital converter
and an impulse counter. Since the determination of β_{eff} requires
an absolute measurement of the power spectral density, the ex-
perimental system was calibrated with a reference signal before
and after each measurement. Through the construction of the co-
herence function it was possible to determine the prompt neutron
flux decay constant α. A more detailed description of these meas-
urements is given in /16/.

Results and Discussions

The results of the measurements in SNEAK-7A and 7B are given in
Table XII. The factor $D = \dfrac{\overline{\nu^2} - \overline{\nu}}{\overline{\nu}^2}$ was taken as $0.815\pm2\%$ for ^{239}Pu.
The calculation of the correction factor g in Eq. (17) was per-
formed in RZ-geometry with the DIXY-program, using the KFKINR cross
section set. The value of g was 1.17 for 7A, and 1.18 for 7B. It is
not sensitive to the assembly, or the cross section data. However,
the influence of the detectors on the flux profile of the assemblies
was not considered.

The results, given in Table XII, agree well with those determined
with the ^{252}Cf-source.

Table XII   Results of β_{eff} Measurements by Noise Analysis

	SNEAK-7A	SNEAK-7B
Reactor power	18.6 watts	45.6 watts
$\alpha_c = \beta_{eff}/l$		
Experiment	$1.65\pm0.17\times10^4$ sec^{-1}	$2.4\pm0.24\times10^4$ sec^{-1}
Calculation (MOXTOT)	1.67×10^4 sec^{-1}	2.07×10^4 sec^{-1}
Calculation (KFKINR)	1.98×10^4 sec^{-1}	2.41×10^4 sec^{-1}
β_{eff}		
Experiment	$0.00421\pm6\%$	$0.00459\pm6\%$
Calculation (MOXTOT)	0.00347	0.00396
Calculation (KFKINR)	0.00359	0.00400

11.4. Discussion of the β_{eff} Results

The experimental and calculated β_{eff} values are summarized in Table XIII. It is interesting that both the apparent ^{252}Cf-worth-method and the noise analysis give practically the same results. Before the comparison with calculated values is discussed, it must be pointed out that the "standard calculation" of β_{eff} used at Karlsruhe is not strictly correct; it uses Keepin's data for the β's and neglects the contribution of ^{241}Pu. It would be appropriate to use the data for $(\nu\beta)$. Therefore, a "modified calculation" was carried out, using the $(\nu\beta)$'s, and including β of ^{241}Pu (which contributes about 1% to the total β_{eff}). These values are slightly larger than the "standard" values (Table XIII).

It is apparent from these results that β values larger than Keepin's should be used. The information on β_8 and β_9 separately could, in principle, be deduced from the pile oscillator measurements. However, the results of these measurements seem to be too high, and it is, therefore, necessary to discuss them in view of their reliability.

The result for $\nu_8\beta_8$ is in agreement with recently published delayed neutron measurements at Los Alamos /17/. However, the high β_9 value for ^{239}Pu seems to disagree with all other available measurements, and we do not suggest that it should be used in β_{eff} calculations. Though we could not clearly identify an error in the experiment, the reactivity peak which appears during the pile oscillator motion with Pu loadings may impair the measurement. It is planned to repeat this experiment with a uniform loading in a later SNEAK assembly.

Thus, the present experiments do not lead to well-established data for β_8 and β_9 separately. However, one can propose as a trial that

Table XIII   Comparison of Measured and Calculated β_{eff} Values

	SNEAK-7A	SNEAK-7B
Experiment		
^{252}Cf-source	0.00416±5%	0.00446±5%
Noise analysis	0.00421±6%	0.00459±6%
Calculation		
Standard method KFKINR	0.00359	0.00400
Modif. method KFKINR	0.00366	0.00406
KFKINR with proposed corrections	0.00407	0.00452

β_8 should be increased by 15%. One can propose, furthermore, a mean β_9 between Keepin's data and the present pile oscillator data, which is about 10% higher than Keepin's value. These proposed data, which are, of course, not well established, lead to β_{eff}'s for SNEAK-7A and 7B which are in good agreement with the measured values (Table XIII). Thus, they may be used until more definite information becomes available.

One word should be said about the influence of delayed neutron
data on the result of a pile oscillator measurement. If an oscil-
lator experiment is analyzed by an inverse kinetics program, the
reactivity is obtained in dollars. However, this result may be
influenced by the delayed neutron data (a_i and λ_i) used in the
program. If the oscillation is sinusoidal, the reactivity ρ ob-
tained in the measurement depends on the flux amplitude $\delta n/n$,
but also on the transfer function $TF(\omega)$ of the reactor

$$\rho \; = \; \frac{\delta n/n}{|TF(\omega)|}$$

Thus, an error in the transfer function, due to delayed neutron
data, leads to an error in the "measured" reactivity. However,
the experimental determination of the transfer function for
SNEAK-7B, as described in Section 10 , verified the magnitude
of the calculated values, so that errors from an incorrect trans-
fer function can be excluded.

This argument holds strictly only for sinusoidal oscillations.
However, it holds, in good approximation, for square wave oscil-
lations used in reactivity worth measurements.

12. Progressive Substitution Experiment

The method of progressive substitution can be used to determine
physics parameters of core compositions built into the central

zone of zoned critical assemblies. The method has been primarily
used in thermal reactors to measure the material buckling. Results
in fast critical assemblies have demonstrated that the method is
applicable for the determination of the material buckling dif-
ferences between the reference and the substituted media with
good accuracy if the reflector savings does not change appreciably
during the measurement.

Description of the Experiment

In the 7B assembly such a substitution measurement was performed
in a stepwise fashion. In the experiment the $U_{nat}O_2$ platelet of
the core zone was replaced by PuO_2-UO_2 (3% PuO_2) of the same
thickness. The substitutions were performed in five successive
steps so that at the end of each step 2, 4, 6, 8, and 16 elements
had been replaced. The cross section of the core with the sub-
stitution steps is shown in Fig. 7. Since no control or shim rods
were in the region in which the substitution was performed (the
shim rod at position 17-17 as shown in Fig. Al-3 was moved before
the experiment) the composition of reference and substituted media
consisted of normal cell platelets only. The corresponding atom
densities are given in Table XIV.

The reactivity change in the assembly for each substitution step
was determined by a calibrated shim rod. A reactivity compensating
amount of core edge elements were removed and the calibration of
the shim rod was redetermined before the next substitution step
was performed. The corresponding changes in the critical radius
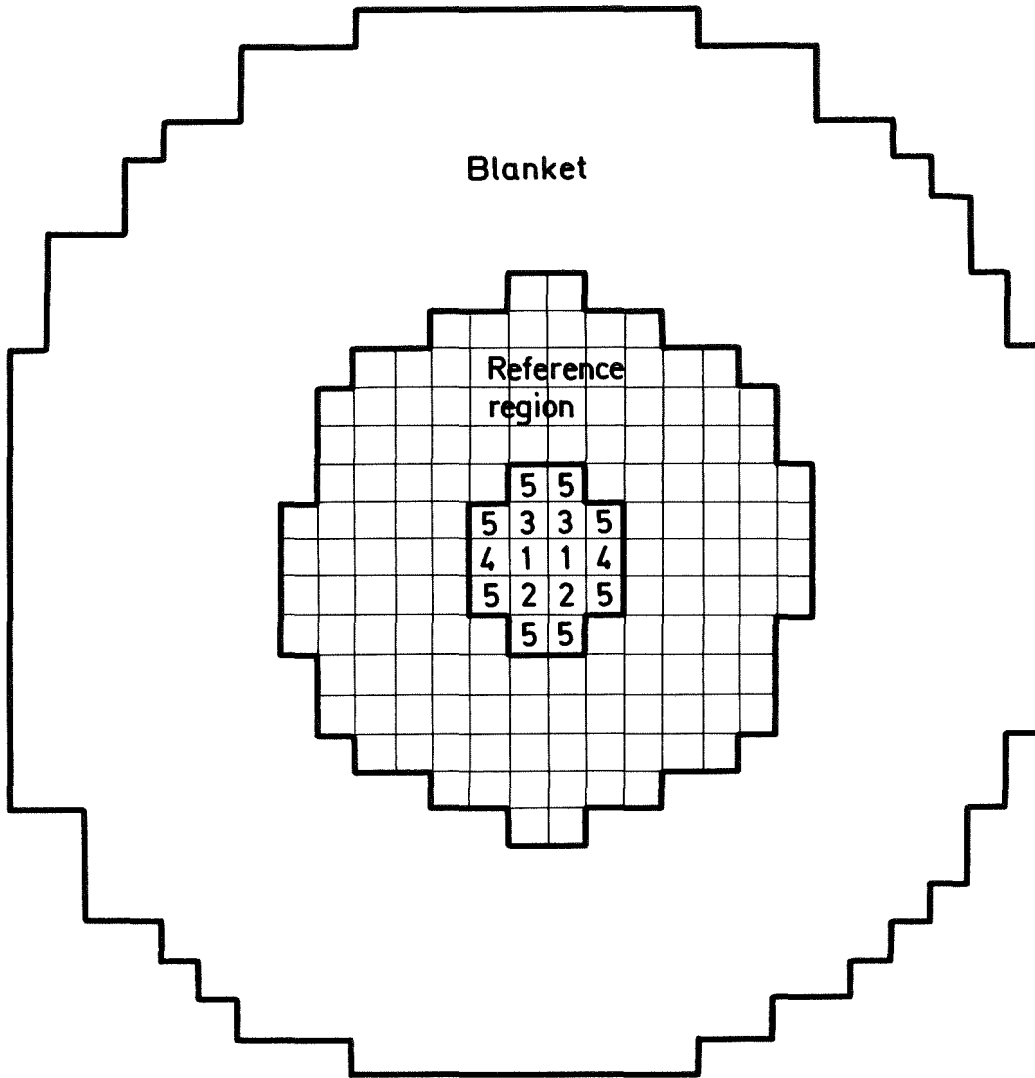determined after each substitution step are given in Table XV.

Fig.7   Cross-section of the SNEAK -7B Core
for the 16-elements substitution

Table XIV   Composition of the Reference and Substituted Media in the SNEAK-7B Assembly for the Substitution Experiment. Atom Densities $\times 10^{-24}/cm^3$

Isotope	Reference $(7B_0)$	Substituted Media $(7B_1)$
Al	.0000120	.0000060
C	.0000659	.0001696
Cr	.0028030	.0027918
Fe	.0099576	.0099902
H	.0000076	--
Mg	.0000053	.0000027
Mn	.0001224	.0001431
Mo	.0000198	.0000231
Nb	.0000090	.0000093
Ni	.0014602	.0014934
O	.0338377	.0332400
^{239}Pu	.0019741	.0021817
^{240}Pu	.0001773	.0002126
^{241}Pu	.0000161	.0000183
^{242}Pu	.0000008	.0000015
Si	.0001197	.0000820
^{235}U	.0001063	.0001040
^{238}U	.0145684	.0141194

Table XV   Experimental Critical Radii for SNEAK-7B Substitution

Number of substituted elements	Substituted zone radius (cm)	Reference zone critical radius R_1 (cm)	Reflector savings δR (cm)	Extrapolated critical radius $R_1 + \delta R$ (cm)
0	0.	37.84	12.00	49.84
2	4.34	37.62	12.04	49.66
4	6.14	37.39	12.05	49.44
6	7.52	37.14	12.06	49.20
8	8.68	36.91	12.05	48.96
16	12.28	36.04	12.05	48.09

Results and Discussions

The spectral-synthesis method, as originally proposed by Storrer /18/ and Kandet /19/, was applied for the interpretation of the experiment. The results obtained are given in Table XVI as a change in the radial buckling between the reference and substituted media. The detailed analysis of the experiment is given by Sotic /20/. The most accurate and reliable value for the difference in the radial buckling obtained in the experiment is

$$(B_r)_{sub} - (B_r)_{ref} = 0.00819 \pm 0.00056 \ (cm^{-1}).$$

Table XVI   Results of Synthesis Calculations for SNEAK-7B Substitution

Number of substitution steps considered	Volume ratio: Substituted to reference V_{sub}/V_{ref}	Buckling difference ΔB_r (cm^{-1})
3	0.040	0.00944 ± 0.00009
4	0.053	0.00926 ± 0.00017
5	0.105	0.00819 ± 0.00056

The value for β_{ref} obtained from the measurements on the reference core, as described in Section 5. of this report, is

$$(B_r)_{ref} = 0.04825\pm0.00003 \ (cm^{-1}).$$

Therefore one obtains for the substituted media a radial component of the buckling of

$$(B_r)_{sub} = 0.05644\pm0.00057 \ (cm^{-1}).$$

According to the investigations performed for various substitution experiments done in the critical assembly MASURCA at Cadarache, France, it is necessary to replace approximately 1/4 to 1/3 of the reference core volume in order to obtain reliable results for the buckling difference. Due to the limited amount of PuO_2-UO_2 (3% PuO_2) platelets available only 1/10 of

the 7B reference core could be substituted in this experiment. It is expected that the true value for ΔB_r, and thus $(B_r)_{sub}$, are smaller. This is supported by calculations with one-dimensional diffusion theory which yields

$$\Delta B_r = 0.00670 \; (cm^{-1}).$$

13. Conclusions

As illustrated by the results in this report the use of the most updated cross section set and calculational methods available significantly improves the description of the two SNEAK-7 assemblies. It is seen that with the KFKINR cross section set the calculated results of the two assemblies are far more consistent than those calculated with the MOXTOT cross section set. The spectral indices calculated with a cross section set based on ENDF/B (Version III) data are surprisingly similar to those of the KFKINR cross section set. This agreement is probably fortuitous as the data in the two sets are different.

The β_{eff} measurements with the ^{252}Cf-source are consistent with those obtained by noise analysis. However, from the reactivity worth measurements, Table XI, the ^{252}Cf-source worth is approximately 7% more overestimated than the worths of the fuel isotopes. This discrepancy probably indicates an inconsistency in the cross section data used to calculate Pu-fueled assemblies. However, a minor part of the discrepancy may also be due to the absolute calibration of the fission rates. Nevertheless the results of many reactivity worth measurements in fast Pu-fueled critical facilities could be better understood if the higher β's proposed in Section 11. were used.

References

/1/   P. Engelmann et al.

        Construction and Experimental Equipment of the Karlsruhe
        Fast Critical Facility, SNEAK
        Kernforschungszentrum Karlsruhe, KFK-471, October 1966

/2/   I.I. Bondarenko et al.

        Group Constants for Nuclear Reactor Calculations

        Consultants Bureau, New York (1964)

/3/   R.B. Kidman et al.

        The Shielding Factor Method of Generating Multigroup
        Cross Sections for Fast Reactor Analysis
        Nucl. Sci. and Eng. 48, 189-201 (1972)

/4/   P.E. Mc Grath and E.A. Fischer

        KAPER, A Computer Program for the Analysis of Experiments
        Performed in Heterogeneous Critical Facilities
        Proc. of the Conf. on Mathematical Models and Computational
        Techniques for Analysis of Nuclear Systems, 9-11 April 1973,
        Ann Arbor, Michigan, CONF-730414

/5/   E. Kiefhaber and J.J. Schmidt

        Evaluation of Fast Critical Experiments Using Recent
        Methods and Data
        Kernforschungszentrum Karlsruhe, KFK-969, Sept. 1970

/6/   E. Kiefhaber

The KFKINR-Set of Group Constants; Nuclear Data Basis
and First Results of its Application to the Recalcu-
lation of Fast-Zero-Power Reactors

Kernforschungszentrum Karlsruhe, KFK-1572, March 1972

/7/   R.B. Kidman and R.E. Schenter

Group Constants for Fast Reactor Calculations

HEDL-TME-71-36, ENDF-143, Hanford Engineering
Development Laboratory, March 1971

/8/   N. Barberger et al.

Analysis of Experiments performed in MASURCA

Conference of the BNES on "The Physics of Fast
Reactor Operation and Design", London 1969

/9/   H. Seufert and D. Stegemann

A Method for Absolute Determination of ^{238}U Capture
Rates in Fast Zero Power Reactors

Nucl. Sci. and Eng. 28, 277-285 (1967)

/10/   E. Korthaus

Messung der Energie- und Ortsabhängigkeit der Neutronen-
einflußfunktion in schnellen kritischen Null-Energie-
Anordnungen

Kernforschungszentrum Karlsruhe, KFK-1141, Mai 1970

/11/   G.R. Keepin

          Physics of Nuclear Kinetics, Addison Wesley New York (1965)

/12/   G. Kussmaul and H. Meister

          Material Worth Measurements with a Fuel-Filled Pile
          Oscillator Rod
          Journal of Nuclear Energy, 25, p. 373 (1971)

/13/   R. Boix-Amat

          Dissertation, Buenos Aires (1971)

/14/   H. Borgwaldt and D. Stegemann

          A Common Theory for Neutronic Noise Analysis Experiments
          in Nuclear Reactors
          Nukleonik 7, 313-325 (1965)

/15/   M. Otsuka and T. Iijima

          Space-Dependent Formula for Rossi-α Measurements

          Nukleonik 7, 488-491 (1965)

/16/   W. Väth

          Messung von β_{eff} an den Anordnungen SNEAK-7A und 7B
          sowie an MASURCA R2 mit der Frequenzanalyse des Reak-
          torrauschens
          Kernforschungszentrum Karlsruhe, KFK-1883 (1974)

/17/   A.E. Evans, M.M. Thorpe, M.S. Krick

        Revised Delayed-Neutron Yield Data

        Nucl. Sci. Eng. 50, 80-83 (1973)

/18/   F. Storrer and J.M. Chaumont

        The Application of Space-Energy Synthesis to the
        Investigation of Fast Multizone Critical Experiments

        in Proc. of the International Conference on Fast Critical
        Experiments and Their Analysis, Oct. 10-13, 1966, Argonne
        National Laboratory, ANL-7320

/19/   R. Kandet

        CEA, Cadarache France, Private Communication (1968)

/20/   O. Sotic

        Interpretation of Substitution Experiments Performed in
        the Fast Critical Facilities MASURCA and SNEAK

        Kernforschungszentrum Karlsruhe, KFK-1930 (1974)

A1. Critical Assembly Geometrical and Composition Data

In this section the matrix plane and cross section for the two clean critical assemblies are given along with the composition data used in the calculational evaluation of the experiments performed in the assemblies.

In Figs. A1.-1 and A1.-3 are shown the matrix planes of the two assemblies with the control rods indicated in their respective positions. The cross sections of the cores, cylinderized for an RZ two-dimensional description, are shown in Figs. A1.-2 and A1.-4, respectively. The fuel elements of the assemblies in SNEAK are suspended vertically with a lattice pitch of 5.44 cm. Platelets of various thicknesses are stacked horizontally within the square fuel element tubes. The cross section of the platelets are (5.077×5.077) cm^2.

The core cell of SNEAK-7A consisted of two platelets, a PuO_2-UO_2 platelet and a graphite platelet, of 0.626 cm and 0.3126 cm thicknesses respectively. The SNEAK-7B core cell consisted of a PuO_2-UO_2 platelet and a UO_2 platelet, of thickness 0.626 cm each. The compositions of these platelets are given in Table A1.-I. These compositions do not represent idealized platelets in that they include the steel of the fuel element tubes and have a reduced density due to the fact that they were stretched to have a surface area corresponding to the lattice pitch squared.

The homogeneous compositions of the cores and blankets of the two assemblies are given in Tables A1.-II to A1.-V. The control rods in these assemblies were loaded with an enriched uranium cell. For homogeneous calculations the uranium control rods were smeared over the assembly core, in SNEAK-7A over an outer ring of the core zone, and in SNEAK-7B over the entire core zone. The compositions of the assemblies with the uranium-loaded control rods homogenized in the above fashion are given in Tables A1.-II and A1.-IV respectively. The average composition of the control rods themselves are given in Table A1.-III and A1.-V. The definition of the two core zones, with and without homogenized uranium control rods, is seen in Fig. A1.-2.

- 68 -

Table Al.-I   Composition of SNEAK Platelets for
Assemblies 7A and 7B
Atom Densities $\times 10^{-24}/cm^3$

Isotope	PuO_2-UO_2	UO_2	Graphite
Al	.0000120	.0000120	
C	.0000626	.0000693	.0780955
Cr	.0028026	.0028034	.0011081
Fe	.0099553	.0099601	.0039549
H	--	.0000156	--
Mg	.0000053	.0000053	--
Mn	.0001224	.0001224	.0000874
Mo	.0000198	.0000198	.0000100
Nb	.0000090	.0000090	.0000085
Ni	.0014600	.0014604	.0005723
O	.0326959	.0349802	--
^{239}Pu	.0039472	--	--
^{240}Pu	.0003546	--	--
^{241}Pu	.0000322	--	--
^{242}Pu	.0000016	--	--
Si	.0001171	.0001222	.0000453
^{235}U	.0000877	.0001249	--
^{238}U	.0119139	.0172242	--

Platelet thicknesses PuO_2-UO_2: 0.626 cm
UO_2:   0.6257 cm
Graphite: 0.3126 cm

Table A1.-II   Regional Compositions in SNEAK-7A
Atom Densities $\times 10^{-24}/cm^3$

Isotope	Inner core zone (pure core material)	Outer core zone	Blanket
Al	.0000080	.0011906	
C	.0260987	.0255387	.0000135
Cr	.0022423	.0022390	.0011080
Fe	.0079713	.0079824	.0039549
Mn	.0001109	.0001178	.0000875
Mo	.0000165	.0000145	.0000100
Nb	.0000089	.0000077	.0000085
Ni	.0011664	.0011818	.0009845
O	.0218462	.0211909	--
^{239}Pu	.0026374	.0023434	--
^{240}Pu	.0002369	.0002105	--
^{241}Pu	.0000215	.0000191	--
^{242}Pu	.0000011	.0000010	--
Si	.0000933	.0000932	.0000453
^{235}U	.0000586	.0002958	.0001624
^{238}U	.0079604	.0080456	.0399401

Table Al.-III   Atom Densities x10^{-24}/cm^3 for the Control
Rods - SNEAK-7A

Isotope	Control rod loaded with PuO_2UO_2	Control rod loaded with uranium
Al	.0000069	.0110350
C	.0218819	.0218280
Cr	.0029907	.0020255
Fe	.0107955	.0073807
Mn	.0001819	.0001600
Mo	.0000056	--
Nb	.0000003	--
Ni	.0015066	.0012258
O	.0180535	.0165945
^{239}Pu	.0021795	--
^{240}Pu	.0001958	--
^{241}Pu	.0000178	--
^{242}Pu	.0000009	--
Si	.0001248	.0000840
^{235}U	.0000484	.0022722
^{238}U	.0065783	.0090673

Table A1.-IV Regional Compositions in SNEAK-7B
Atom Densities $\times 10^{-24}/cm^3$

Isotope	Core	Blanket
Al	.0012112	--
C	.0000631	.0000135
Cr	.0027560	.0011080
Fe	.0098021	.0039549
H	.0000071	--
Mg	.0000095	--
Mn	.0000646	.0000875
Mo	.0000184	.0000010
Nb	.0000084	.0000085
Ni	.0014594	.0009845
O	.0331936	--
^{239}Pu	.0018312	--
^{240}Pu	.0001645	--
^{241}Pu	.0000149	--
^{242}Pu	.0000007	--
Si	.0001174	.0000453
^{235}U	.0002663	.0001624
^{238}U	.0145794	.0399401

Table A1.-V   Atom Densities for the Pure Core Material
and the Control Rods in SNEAK-7B
Atom Densities $\times 10^{-24}/cm^3$

Isotope	Pure core material	Control rods
Al	.0000120	.0165823
C	.0000659	.0000264
Cr	.0028030	.0021535
Fe	.0099576	.0078086
H	.0000076	--
Mg	.0000053	.0000631
Mn	.0001224	.0001585
Mo	.0000198	--
Nb	.0000090	--
Ni	.0014602	.0014496
O	.0338377	.0249366
^{239}Pu	.0019741	--
^{240}Pu	.0001773	--
^{241}Pu	.0000161	--
^{242}Pu	.0000008	--
Si	.0001197	.0000888
^{235}U	.0001063	.0023172
^{238}U	.0145684	.0147206

A2. Description of the Assemblies for Basic Analysis as Spheres

Equivalent spherical models have been defined for the two SNEAK-7
assemblies for the purpose of providing a system amenable to anal-
ysis with one-dimensional programs. The homogeneous spherical mo-
dels were obtained by iterating on the radius in a one-dimensional
spherical diffusion calculation to obtain a specified k_{eff}. The
k_{eff} was obtained from the RZ two-dimensional diffusion calcula-
tion as described in Section 4. It was corrected for cylindriza-
tion, control rod homogenization, and heterogeneity effects. The
core composition in the spherical model is that of the "pure" core
for SNEAK-7A, but includes the control rods for SNEAK-7B (see
Table A1.-II and A1.-V of Appendix A1). The resultant models for
the two assemblies is given below in the table.

Models for Basic Analysis as a Sphere

	SNEAK-7A	SNEAK-7B
Core radius	28.50 cm	40.64 cm
Reflector thickness	30.0 cm	30.0 cm
Code	Diffusion or S_6	Diffusion or S_6
Mesh	35 intervals, core	45 intervals, core
	20 intervals, reflector	20 intervals, reflector

The experimental results for the spectral indices and the small-
sample reactivity worths were corrected for the spherical models
and are given in Tables A2.-I and A2.-II.

Table A2.-I   Spectral Indices at the Core Center

	Experimental value (cell averaged)	Correction for homogeneous, spherical core	Value for the equivalent homog. sphere
SNEAK-7A			
σ_{f8}/σ_{f5}	$0.0449\pm3\%$	-0.3%	0.0448
σ_{f9}/σ_{f5}	$0.984\pm3\%$	-0.7%	0.977
σ_{c8}/σ_{f5}	$0.138\pm3\%$	-0.3%	0.138
SNEAK-7B			
σ_{f8}/σ_{f5}	$0.0328\pm2\%$	$+0.5\%$	0.0330
σ_{f9}/σ_{f5}	$0.975\pm2\%$	-0.2%	0.973
σ_{c8}/σ_{f5}	$0.132\pm3\%$	-0.6%	0.131

Table A2.-II   Material Worths at the Core Center

Material	Sample thickness, g/cm^2	Reactivity coefficient, 10^{-5} $\Delta k/k$ / mole			
		SNEAK-7A		SNEAK-7B	
		measured	infinitely small sample in the equivalent sphere	measured	infinitely small sample in the equivalent sphere
^{235}U	0.17	189.8±3%	208.3	118.9±2%	121.2
^{238}U	5.7	− 9.40±3%	− 11.04	− 6.38±2%	− 6.90
^{239}Pu	0.095	+260 ±3%	287	−−	−−
	0.19	−−	−−	162.0±2%	166.9
^{240}Pu	0.12	+ 62.0 ±8%	70.4	28.8±10%	30.8
^{10}B	0.024	−198.2 ±2%	−226	− 82.8±2%	− 90.3
Ta	1.67	− 56.2 ±2%	− 87.2	− 23.2±2%	− 29.8
Eu$_2$O$_3$	0.165	−441 ±2%	−492	−164.7±3%	−174
Fe	1.15	− 1.93±10%	− 2.24	−−	−−
	2.30	−−	−−	− 1.34±5%	− 1.42

A3. Reaction Rate Traverses

The fission rate traverses of ^{239}Pu and ^{238}U were measured in the
axial and radial directions with chambers of type FC4 (20th Century
Electronics) having a 6 mm outer diameter and 25 mm active length.
In SNEAK-7A the axial traverses were measured at position (17-19)
of Fig. A1.-1 in Appendix A1. The radial traverses were performed
along position (X-19). The accuracy of these chamber measurements
is estimated to be approximately 0.3% in the core region and slightly
less than 1% in the blanket. Since the traverse measurements were
used to determine the material buckling (see Section 5.) and the
normalization integral for the evaluation of β_{eff} (see Section 11.)
an additional axial measurement was performed in the edge element
at position (22-19) to check the separability of the flux. The
measurement in this position yielded essentially the same form as
that from the central element. Therefore, to a good approximation,
the flux was separable in the radial and axial directions. The
axial and radial traverses were also measured with foils by the
activation method. These results for SNEAK-7A are given in Figs.
A3.-1 and A3.-2 together with the calculated traverses. The calcu-
lated traverses are from two-dimensional diffusion theory calcula-
tions with the MOXTOT cross section set. The axial traverses were
calculated in RZ-geometry and the radial in XY-geometry in which
the control rods were considered in their respective positions (i.e.
not smeared over the core). Since corrections for heterogeneity and
transport effects are throughout small, they were neglected.

In the core region the chamber measurements lie somewhat higher than
the calculations. In addition the majority of the foil measurements
are consistent with the chamber measurements. However, a few of the
foil measurements are clearly not consistent with the other measure-
ments. They probably have a larger measurement error than assumed.

In the blanket the foil measurements lie under the chamber
measurements. This can possibly be explained qualitatively as
an effect of streaming in the channel for the chamber measure-
ment.

Similar traverse measurements were also performed in SNEAK-7B.
The axial traverses were measured in position (17-20) of Fig.
A1.-3 in Appendix A1. and the radial traverses in position (X-19).
The calculations were performed as in the SNEAK-7A evaluation.
They were repeated however with the KFKINR cross section set.
The results of the calculations and measurements are given in
Figs. A3.-3 and A3.-4. One sees that the results are very similar
to those of SNEAK-7A. With the KFKINR cross section set the cal-
culation lies slightly higher in the outer portion of the core,
and in the blanket, than that calculated with the MOXTOT set.
This means that with the KFKINR cross section set one would cal-
culate a larger normalization integral than with the MOXTOT set.

The ^{238}U capture rate was measured in the same axial and radial
positions as the fission rate traverses in SNEAK-7B. The measure-
ment was performed with enriched uranium foils (20% ^{235}U) between
the platelets of the core. The gamma spectra, between approxima-
tely 150 and 300 keV, of the irradiated foils were measured with
a 20 cm^3 Ge(Li)-detector. To determine the capture rate the sur-
face area of the 277 keV-line of ^{239}Np and the 185 keV-line of
^{235}U were utilized. The results of these measurements are shown
in Figs. A3.-5 and A3.-6 for the axial and radial traverses, res-
pectively. The calculations were performed in the same manner as
the fission rate traverse calculations. One sees the same general
trend in the agreement between the measurements and calculations
as in the fission rate traverses.

A4. Reactivity Worth Traverses

The radial and axial space dependence of the neutron impor-
tance function was determined by measuring the apparent reac-
tivity effect of ^{252}Cf-source neutrons in both assemblies.
This was accomplished by oscillating a ^{252}Cf-source in a
radial and axial channel of the core. The apparent reactivity
effect of the Cf-source was obtained from two measurements as
explained for the measurements described in Section 8. In ad-
dition to the Cf-source measurements radial reactivity tra-
verses were also performed in both assemblies with a ^{10}B and
a ^{239}Pu sample.

The results of these measurements and their analysis with two-
dimensional diffusion theory with the MOXTOT cross section set
are shown in Figs. A4.-1 to A4.-6. In general the agreement
between the measurements and calculations is quite good. Of
the reactivity worth samples the ^{239}Pu measurements show the
greatest discrepancy with calculation. The calculations to-
ward the core-blanket interface underestimate the ^{239}Pu reac-
tivity worth. The errors quoted in the measurements of the
traverses are from the statistical fluctuations in the posi-
tion of the calibrated automatic control rod.
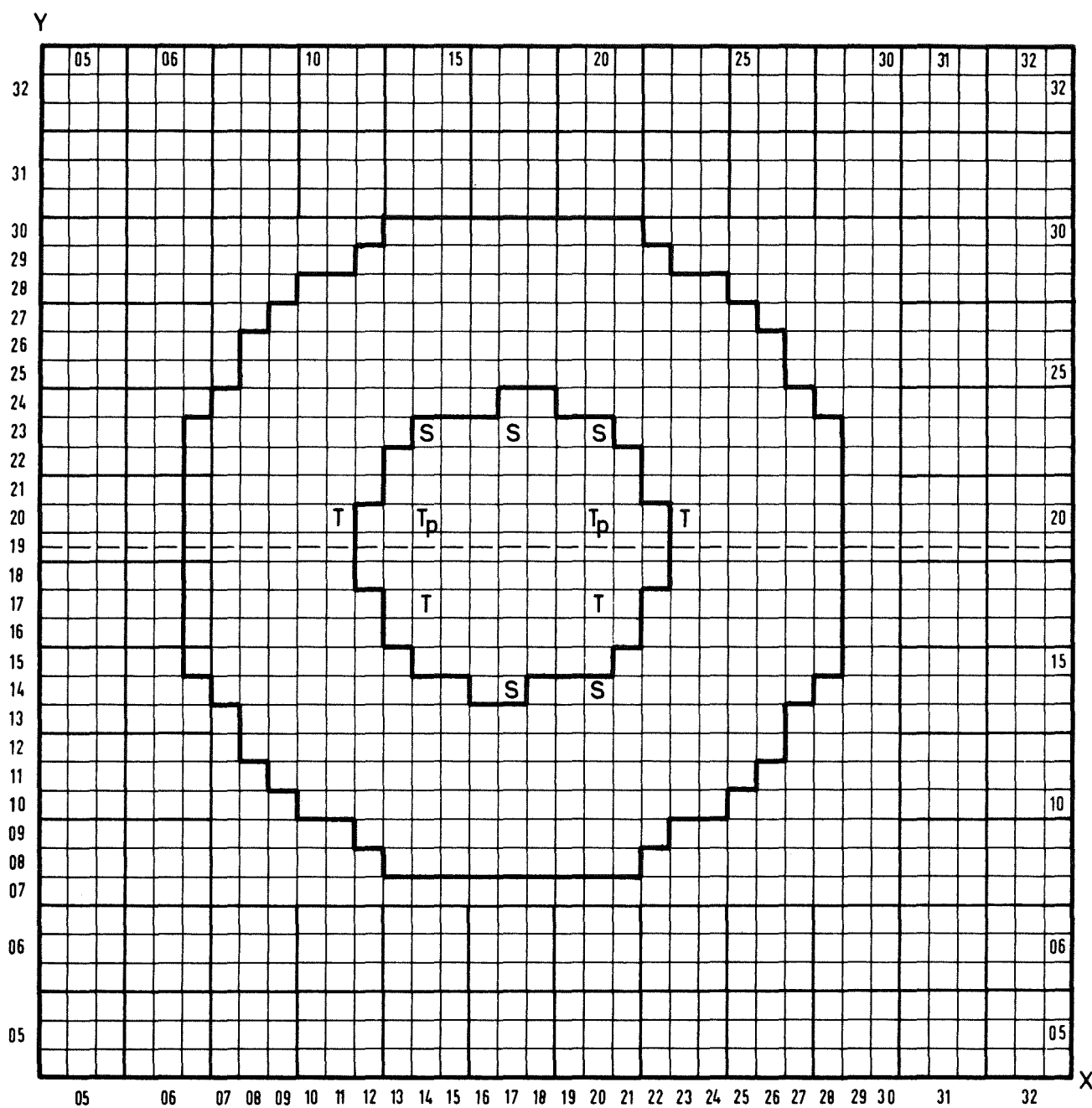
SNEAK - 7A   Core map

T_p PuO_2 - UO_2 loaded shim rod
T   U-loaded shim rod
S   U-loaded safety rod
Lattice pitch : 5.44 cm
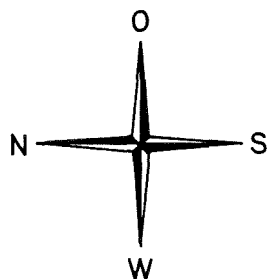
Fig. A1-1
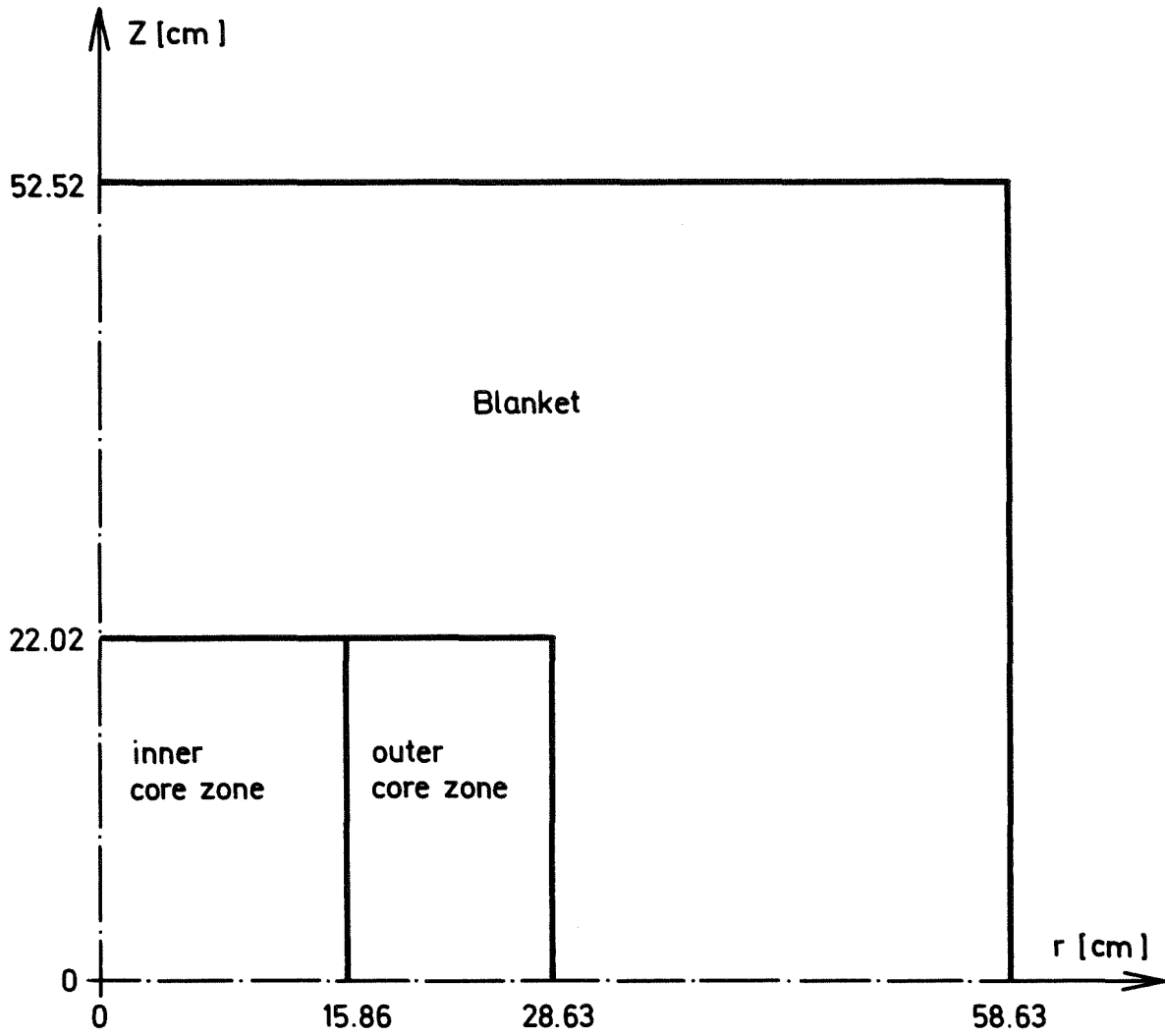
Fig. A1-2   RZ-model for assembly SNEAK-7A
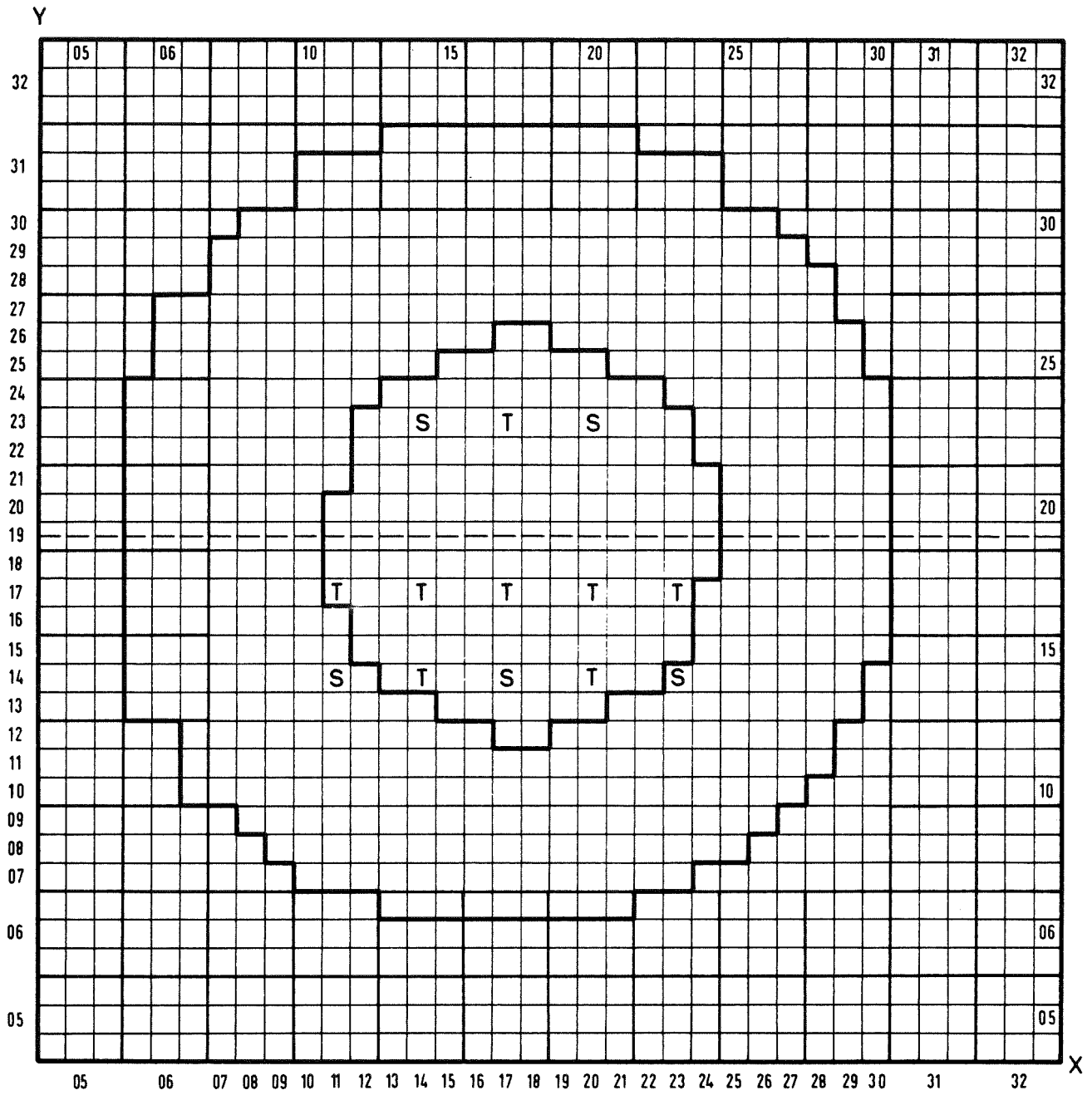
SNEAK-7B   Core map

T   shim rod
S   safety rod
Lattice pitch : 5.44 cm
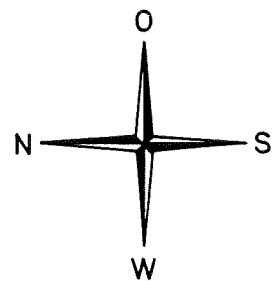
Fig. A1-3
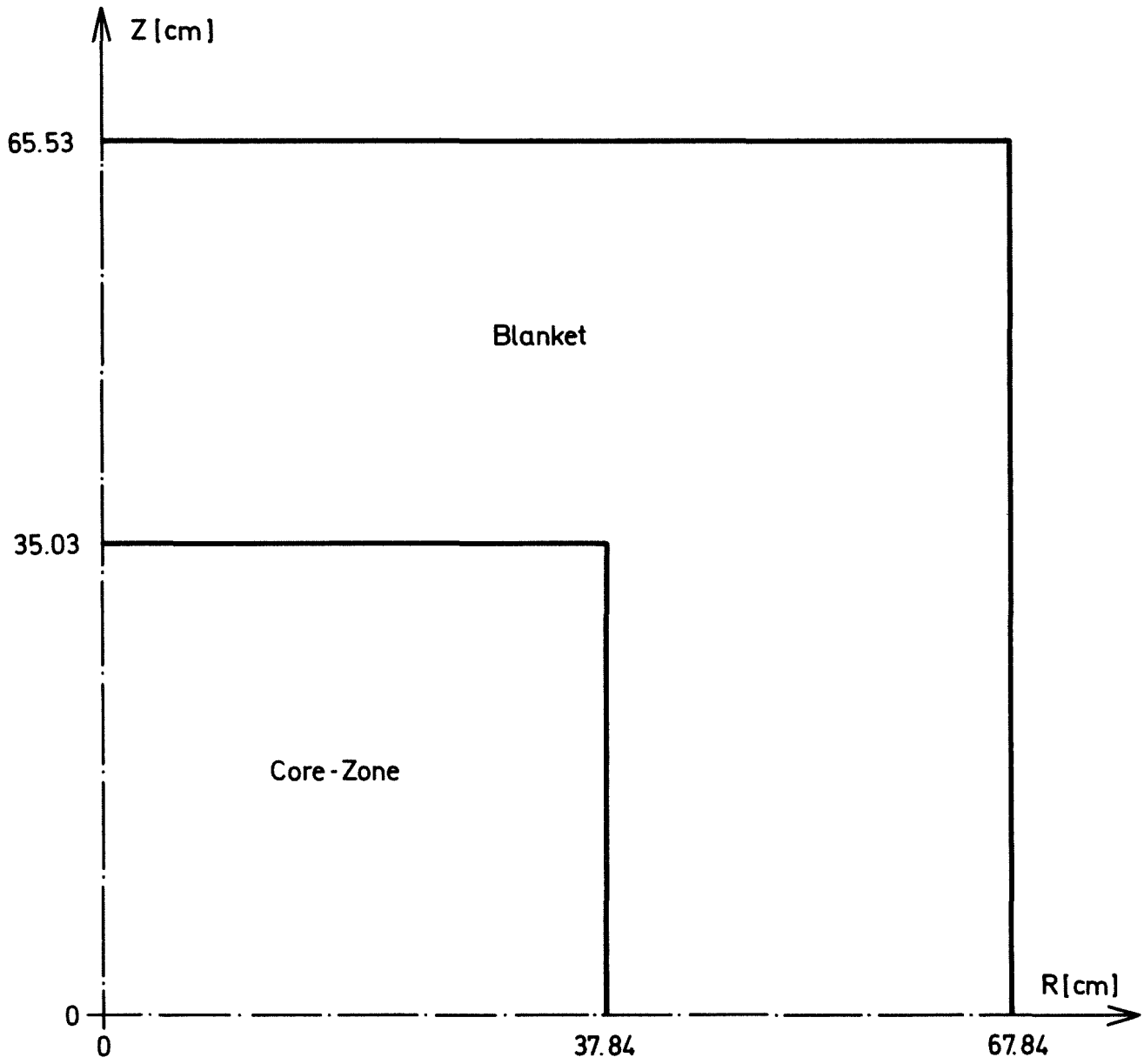
Fig. A1-4   RZ-model for assembly SNEAK-7B
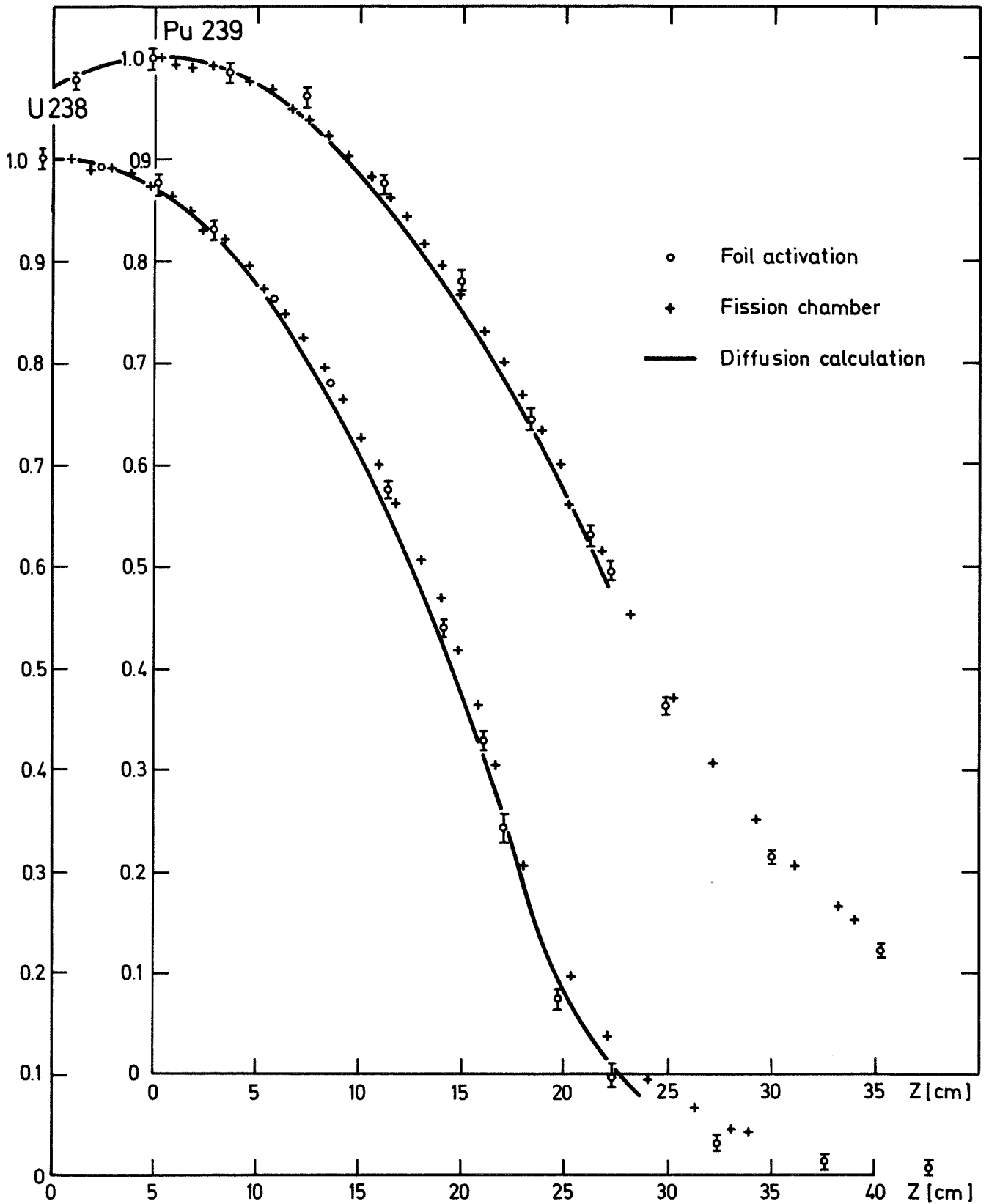
Fig. A3-1   Axial fission rate traverses SNEAK-7A, Pu 239 and U238
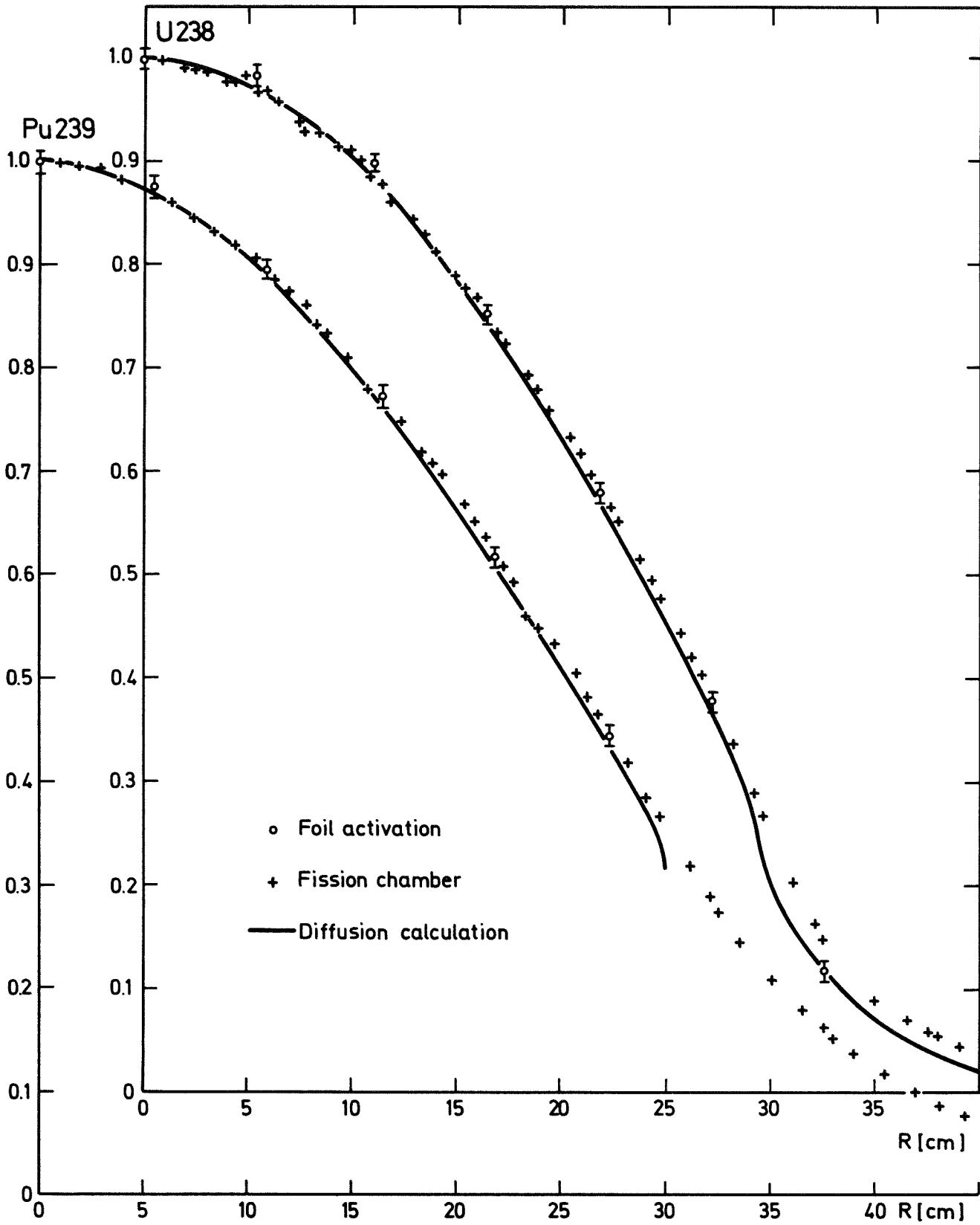
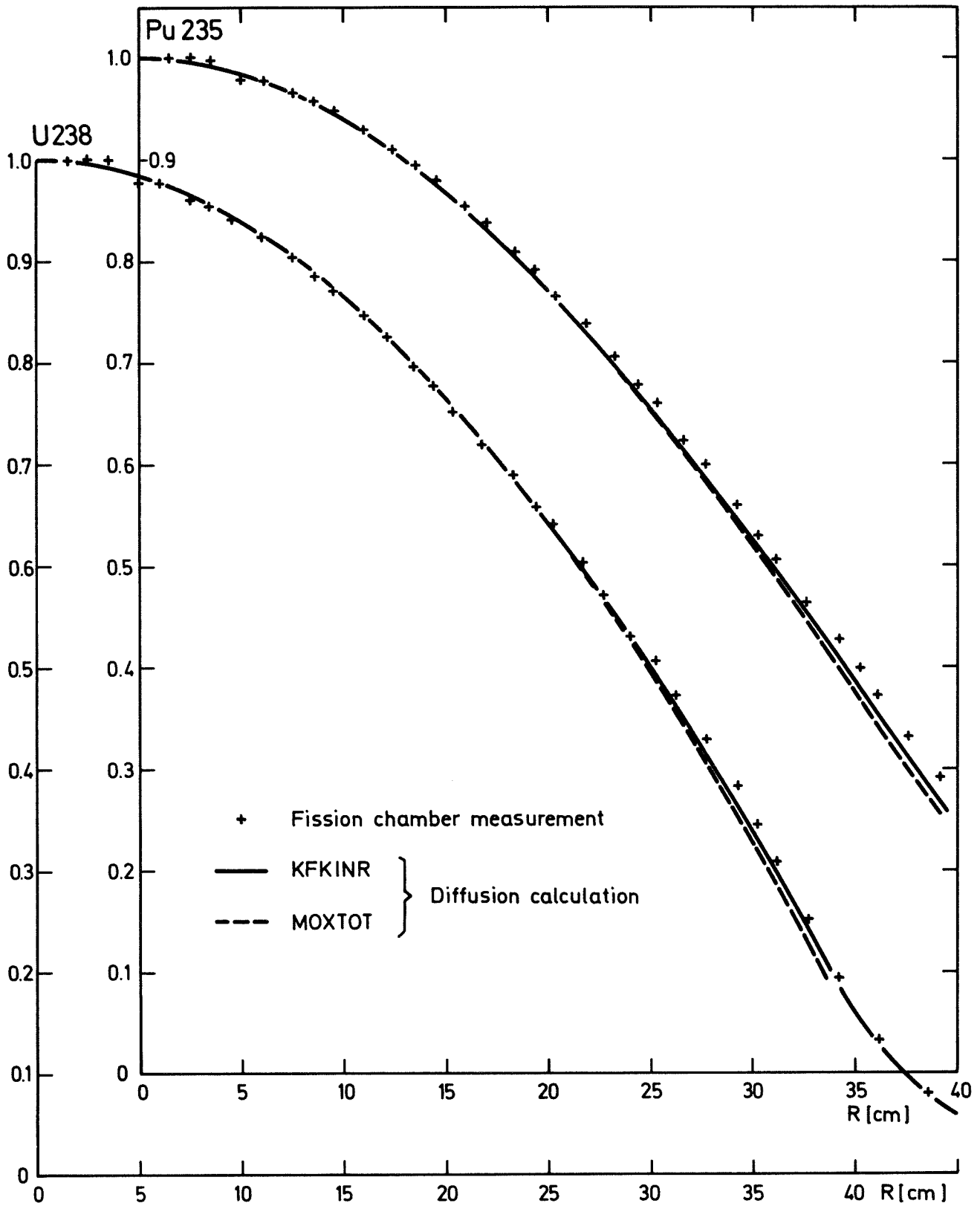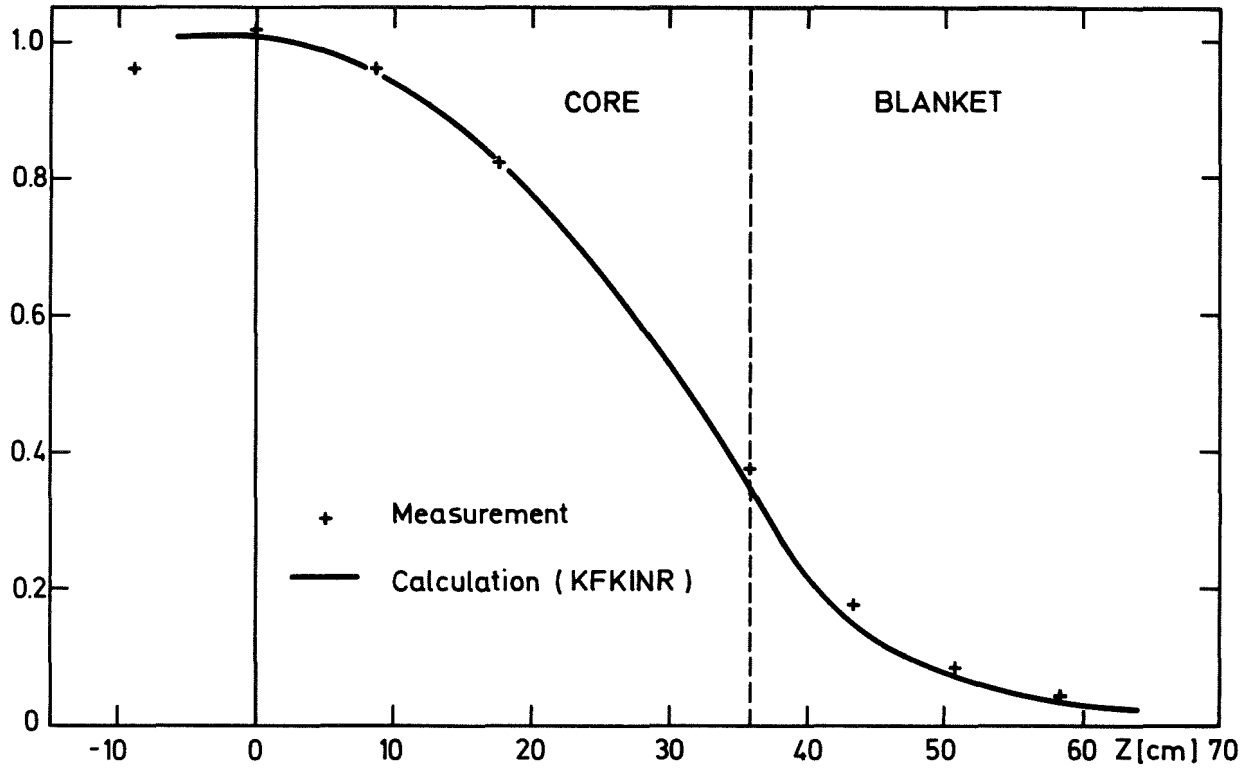Fig. A3-2   Radial fission rate traverses SNEAK-7A, Pu 239 and U 238
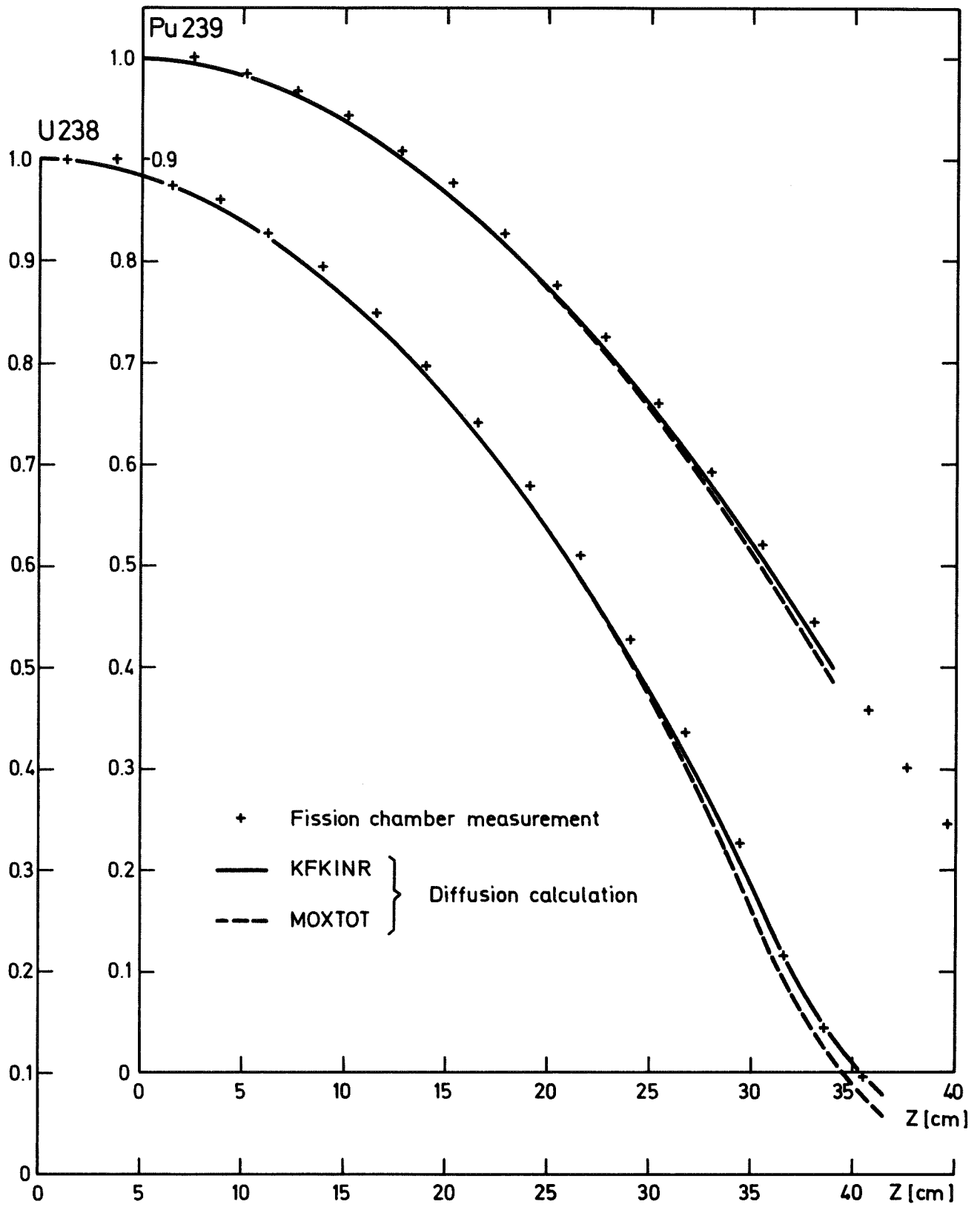
Fig. A3-3   Axial fission rate traverses SNEAK-7B, Pu 239 and U 238

Fig. A3-4   Radial fission rate traverses SNEAK-7B, Pu239 and U238

Fig. A3-5   Axial U238 capture rate traverse, SNEAK-7B
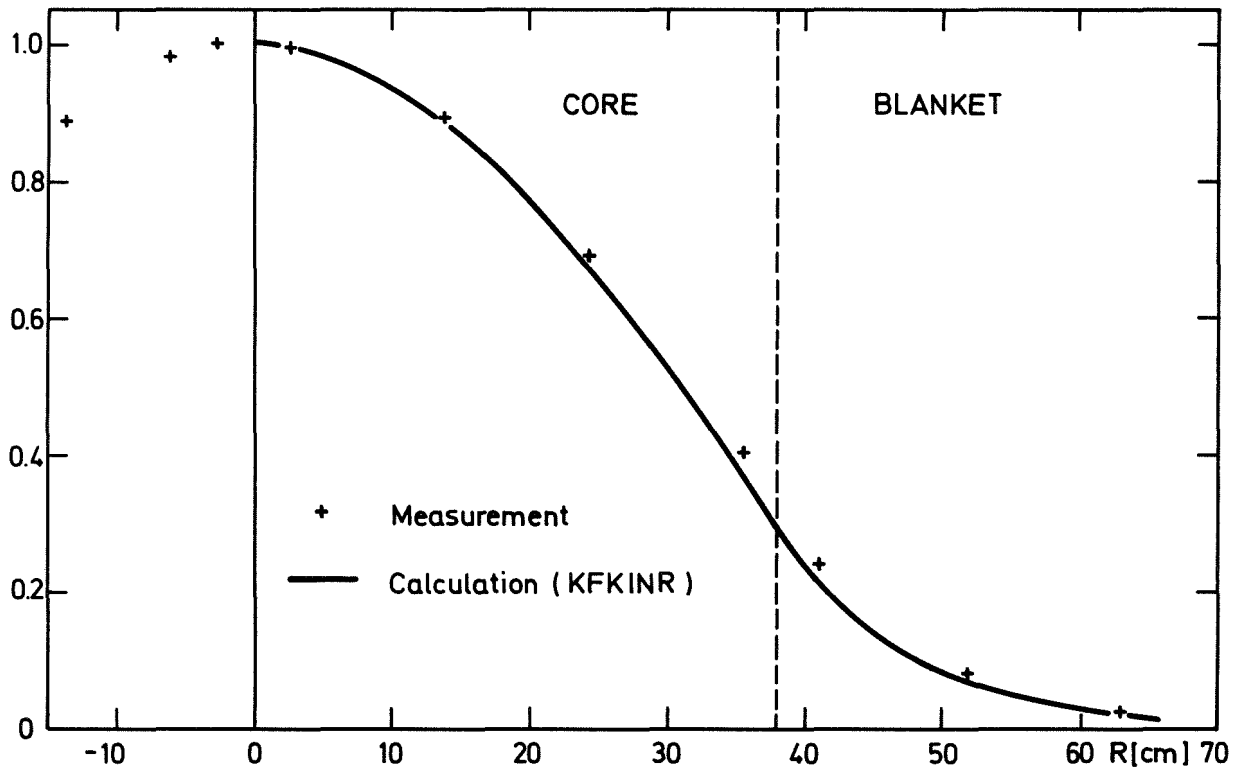
Fig. A3-6   Radial U238 capture rate traverse, SNEAK-7B
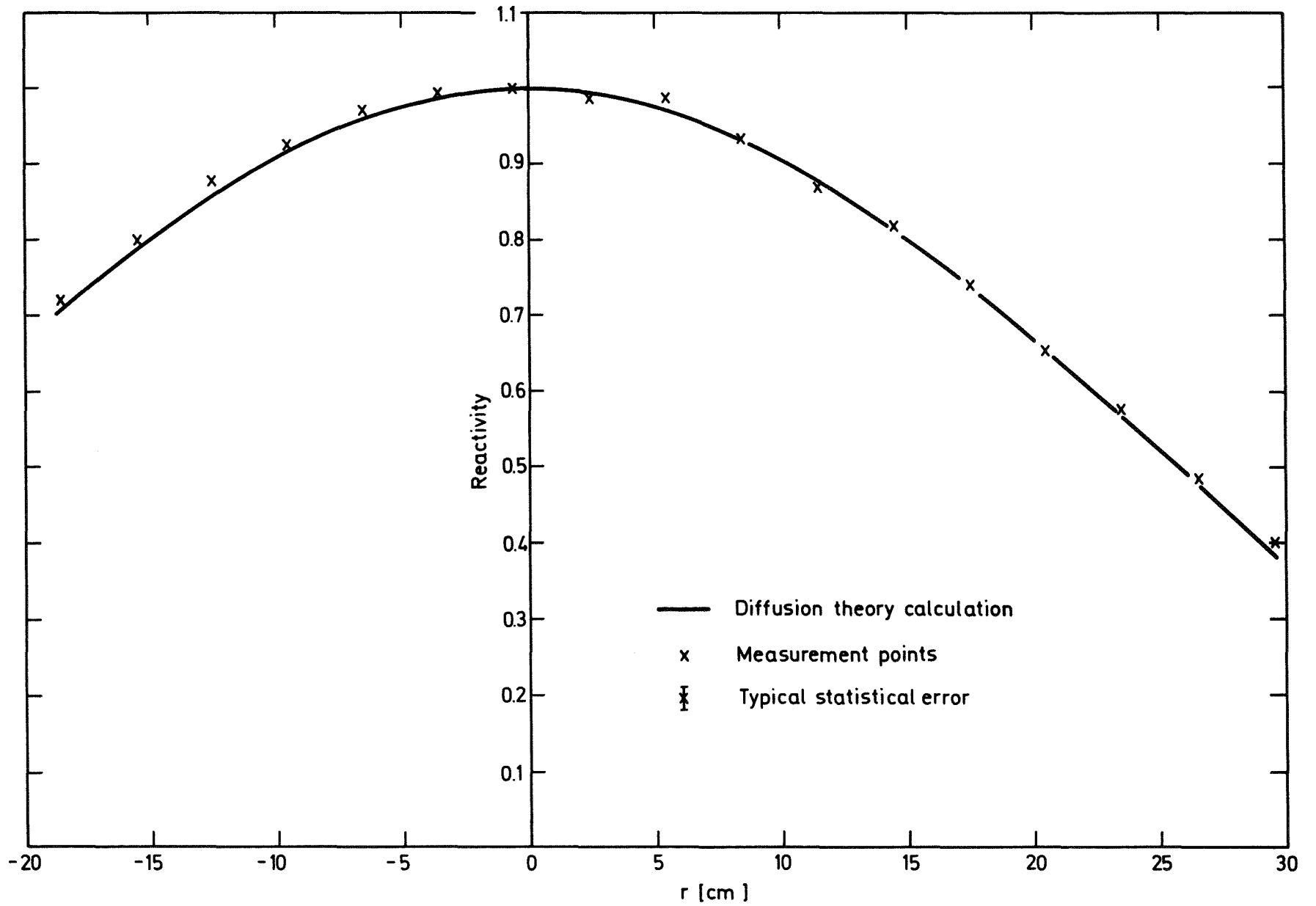
Fig. A4-1   Radial Cf 252 - traverse (North - south direction) SNEAK - 7A
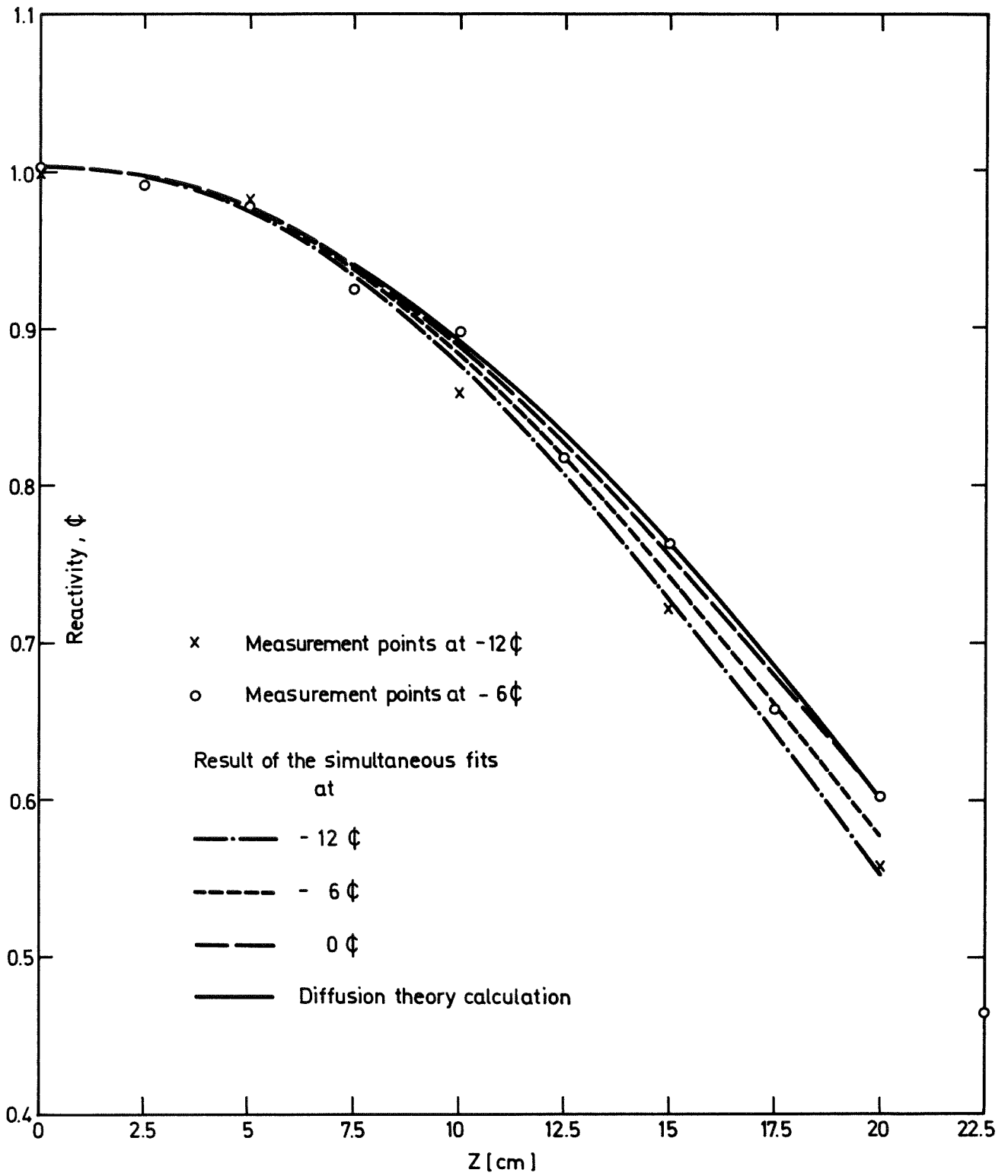
Fig. A4-2   Axial Cf 252 - traverse SNEAK-7A
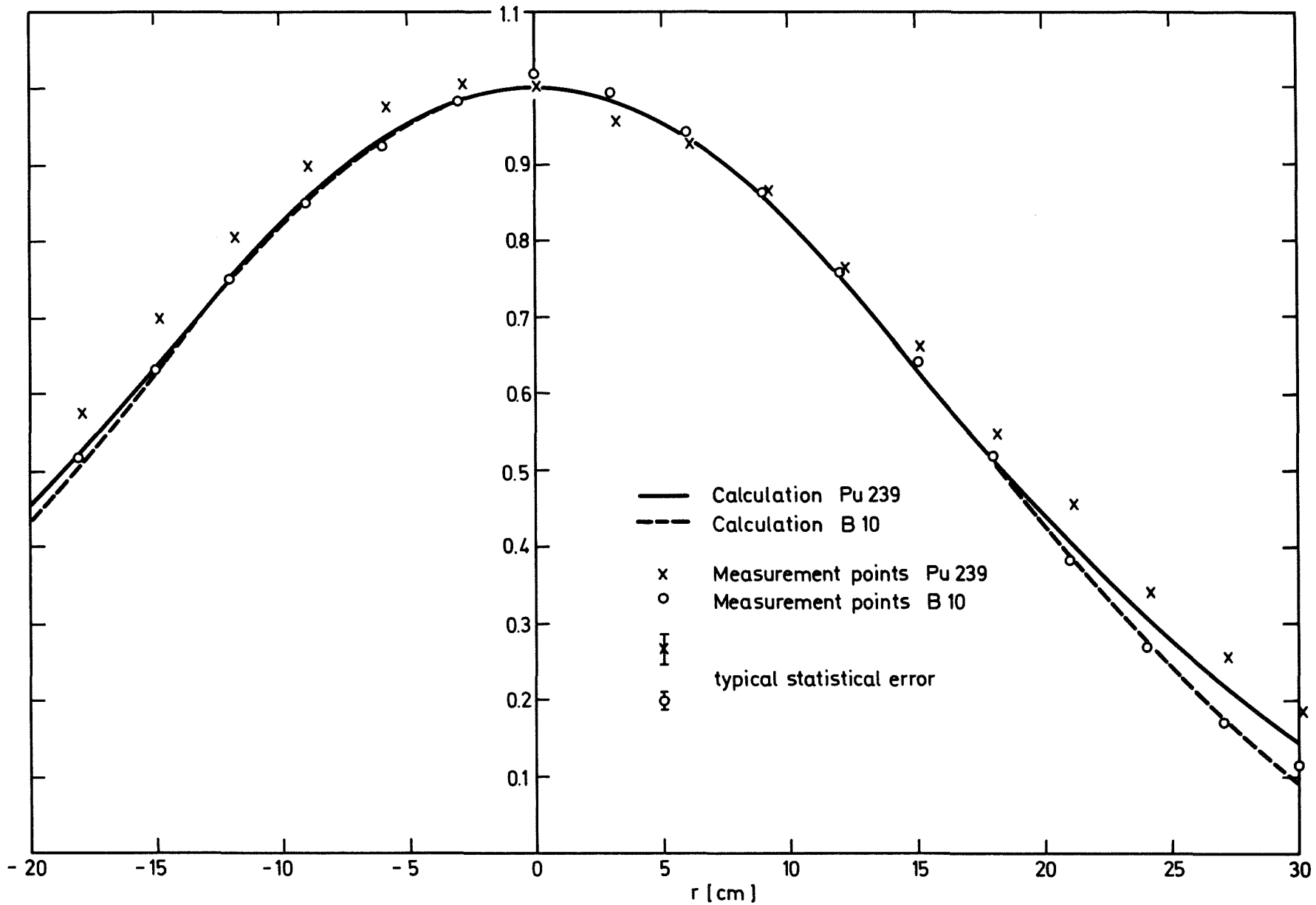
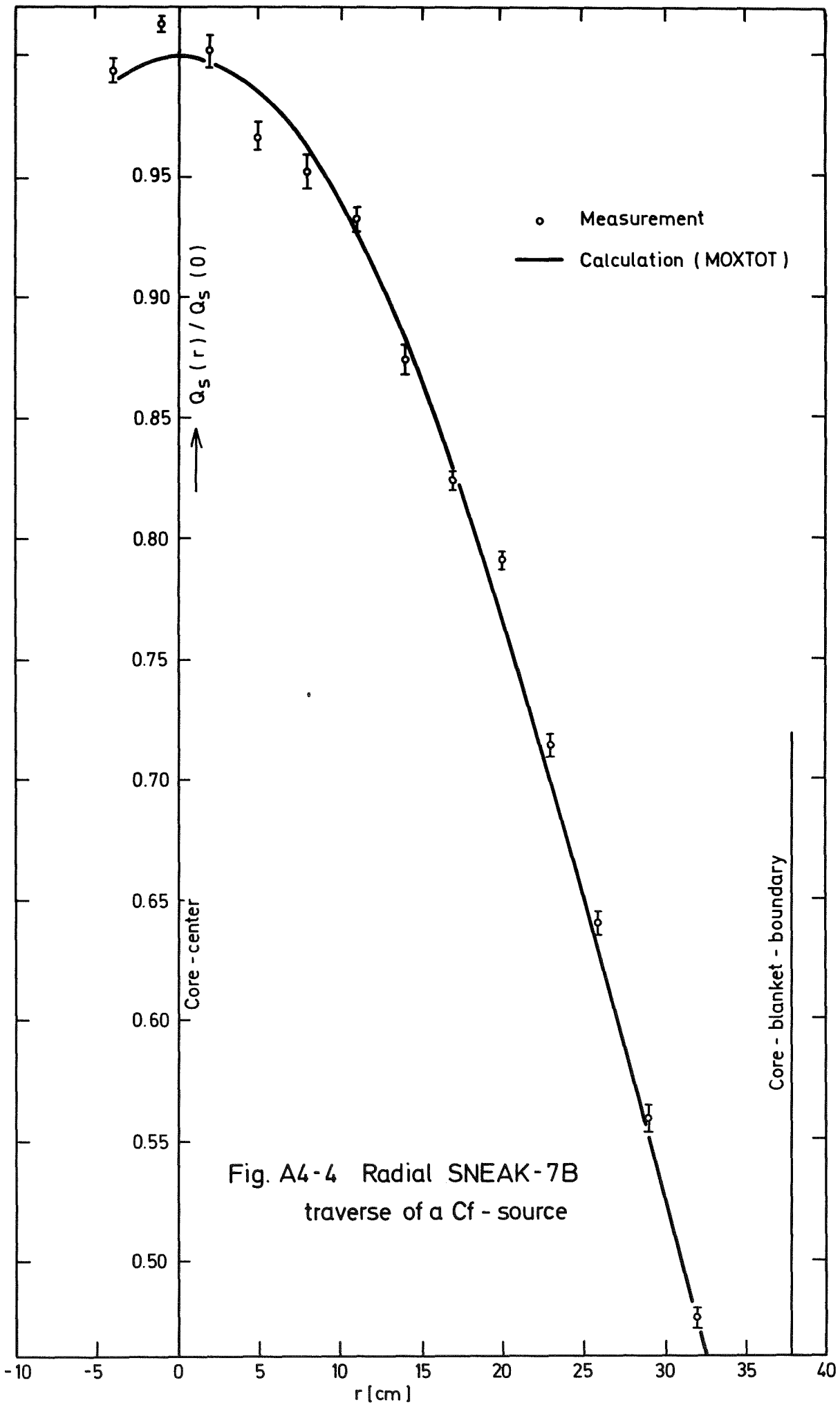Fig. A4-3　Radial materialworth - traverses　(North - south direction) SNEAK - 7A

Fig. A4-4   Radial SNEAK-7B
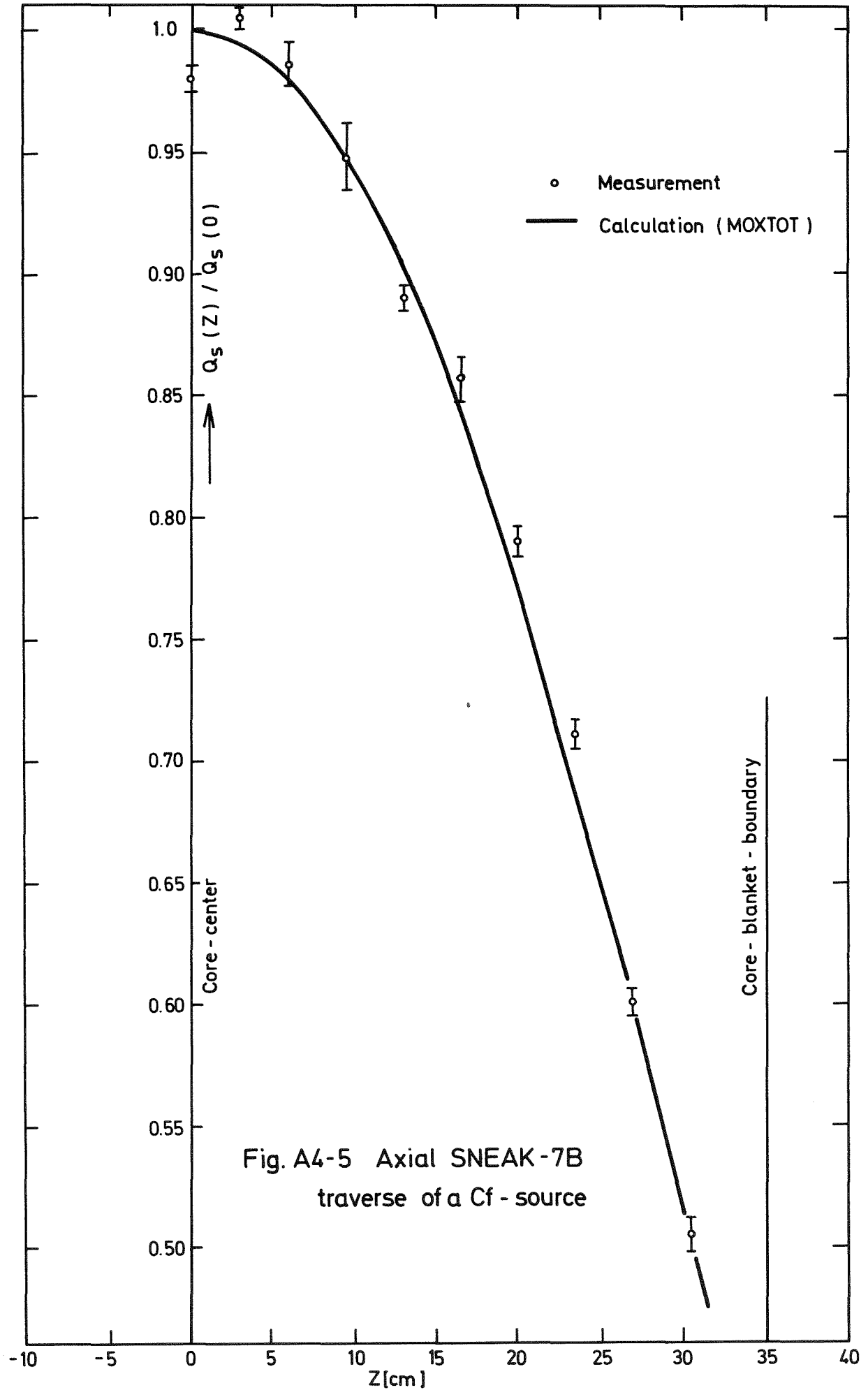traverse of a Cf - source

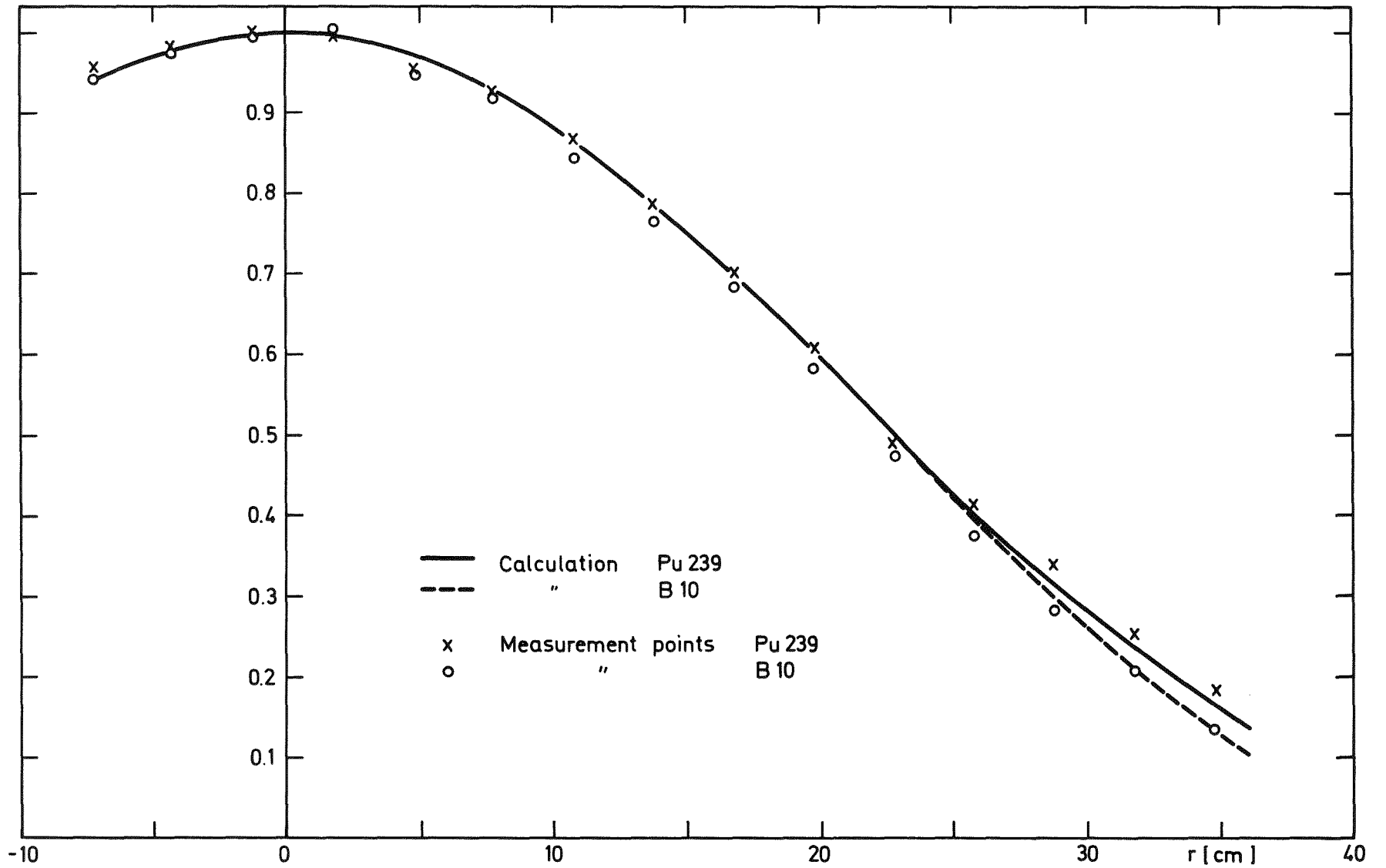Fig. A4-5   Axial SNEAK-7B
traverse of a Cf - source

Fig. A4-6   Radial material worth traverses (North - south direction) SNEAK-7 B